

## MODELLING OF WETTABILITY ALTERATION PROCESSES IN CARBONATE OIL RESERVOIRS

LIPING YU, HANS KLEPPE, TERJE KAARSTAD  
AND SVEIN M. SKJAEVELAND

University of Stavanger, NO-4036 Stavanger, Norway

STEINAR EVJE\* AND INGEBRET FJELDE

International Research Institute of Stavanger (IRIS)  
Prof. Olav Hanssensvei 15, NO-4068 Stavanger, Norway

(Communicated by Kenneth Karlsen)

**ABSTRACT.** Previous studies have shown that seawater may alter the wettability in the direction of more water-wet conditions in carbonate reservoirs. The reason for this is that ions from the salt (sulphat, magnesium, calcium, etc) can create a wettability alteration toward more water-wet conditions as salt is absorbed on the rock.

In order to initiate a more systematic study of this phenomenon a 1-D mathematical model relevant for spontaneous imbibition is formulated. The model represents a core plug on laboratory scale where a general wettability alteration (WA) agent is included. Relative permeability and capillary pressure curves are obtained via interpolation between two sets of curves corresponding to oil-wet and water-wet conditions. This interpolation depends on the adsorption isotherm in such a way that when no adsorption of the WA agent has taken place, oil-wet conditions prevail. However, as the adsorption of this agent takes place, gradually there is a shift towards more water-wet conditions. Hence, the basic mechanism that adsorption of the WA agent is responsible for the wettability alteration, is naturally captured by the model.

Conservation of mass of oil, water, and the WA agent, combined with Darcy's law, yield a 2x2 system of coupled parabolic convection-diffusion equations, one equation for the water phase and another for the concentration of the WA agent. The model describes the interactions between gravity and capillarity when initial oil-wet core experiences a wettability alteration towards more water-wet conditions due to the spreading of the WA agent by molecular diffusion. Basic properties of the model are studied by considering a discrete version. Numerical computations are performed to explore the role of molecular diffusion of the WA agent into the core plug, the balance between gravity and capillary forces, and dynamic wettability alteration versus permanent wetting states. In particular, a new and characteristic oil-bank is observed. This is due to incorporation of dynamic wettability alteration and cannot be seen for case with permanent wetting characteristics. More precisely, the phenomenon is caused by a cross-diffusion term appearing in capillary diffusion term.

---

2000 *Mathematics Subject Classification.* 76S05, 76R50, 76R05, 65M12, 35L65, 35K65.

*Key words and phrases.* physico-chemical processes, porous media flow, wettability alteration, spontaneous imbibition, capillary diffusion, molecular diffusion, adsorption, convection-diffusion equations, cross-diffusion.

The authors acknowledge ConocoPhillips and the Ekofisk Coventurers, including TOTAL, ENI, Hydro, Statoil and Petoro, for supporting the work through the research center COREC.

\*Corresponding author.

**1. Introduction.** Seawater has been injected into the naturally fractured Ekofisk chalk reservoir in the North Sea for nearly 20 years with great success. Many laboratory studies of spontaneous imbibition test with chalk cores indicate that seawater has the potential to improve oil recovery. Especially it has been observed that the sulphate ions in seawater have a catalytic effect on wettability alteration processes [1, 2, 3, 4, 5, 6, 7, 8, 9]. In these studies the sulphate ions in seawater were observed as the key factor leading to wettability alteration towards more water-wetness. The mechanism to explain the experimental results is then suggested as follows:

Sulphate can adsorb onto the chalk surface and make the surface less positively charged. The desorption of negative charged acidic material on the surface becomes easier with less electrostatic interactions between oil components and the chalk surface. Further studies show that calcium and magnesium may cooperate with sulphate ions to contribute to this wettability alteration process. Thus, there is a wealth of experimental data which require systematic analysis. In order to exploit fully the data that is generated through experiments there is a need for developing mathematical models which take into account dynamic wettability alteration.

The objective of this paper is to build a 1-D model to simulate the laboratory spontaneous imbibition experiments of seawater into preferentially oil-wet cores, owing to alteration of flow parameters (in terms of relative permeability and capillary pressure curves) caused by a general wettability alteration (WA) agent. This agent may represent ions from sulphate, calcium, magnesium, et al. Relative permeability and capillary pressure curves are obtained via a natural interpolation between two given sets of relative permeability curves ( $k_r^{ow}, k_r^{ww}$ ) and capillary pressure curves ( $P_c^{ow}, P_c^{ww}$ ) corresponding to oil-wet and water-wet conditions. This interpolation depends on the adsorption isotherm in such a way that when no adsorption of the WA agent has taken place, oil-wet conditions prevail. However, as the adsorption of this agent takes place, gradually there is a shift towards more water-wet conditions. Hence, the basic mechanism that adsorption of the WA agent is responsible for the wettability alteration, is naturally captured by the model.

Conservation of mass, combined with Darcy's law, then yield a model of the form (dimensionless form)

$$\begin{aligned} s_t + f(s, c)_x &= \varepsilon([-\lambda_o f](s, c)P_c(s, c)_x) \\ (sc + a(c))_t + (cf(s, c))_x &= \delta(D(s)c_x) + \varepsilon(c[-\lambda_o f](s, c)P_c(s, c)_x), \end{aligned} \quad (1)$$

where  $s$  is water saturation,  $c$  concentration of WA agent,  $f$  is fractional flow function,  $\lambda_o$  is oil mobility,  $P_c$  capillary pressure,  $D(s)$  molecular diffusion coefficient,  $a(c)$  adsorption isotherm, whereas  $\varepsilon$  and  $\delta$  are dimensionless characteristic numbers. Models of the form (1) have been studied extensively before in connection with for example polymer and surfactant flooding. A nice overview of this activity is given in the book [10] which also includes a comprehensive reference list. However, common for most of this work is that focus is on reservoir scale displacement phenomena. That is, the dimensionless parameter  $\varepsilon \sim \frac{1}{L}$ , where  $L$  represents reservoir length, becomes small ( $\varepsilon \ll 1$ ) and diffusion terms (capillary and molecular diffusion) are neglected. The resulting model then is a system of conservation laws of the form

$$\begin{aligned} s_t + f(s, c)_x &= 0 \\ (sc + a(c))_t + (cf(s, c))_x &= 0, \end{aligned} \quad (2)$$

for which analytical solutions can be constructed, see e.g. [11, 12, 10]. In contrast, since the focus of this work is on modelling of spontaneous imbibition due to wettability alteration on laboratory scale, the capillary diffusion and molecular diffusion terms in (1) cannot be neglected. In fact, these terms are crucial for the performance of the whole imbibition process and a main objective of the present work is to gain a more accurate understanding of the impact from these terms.

In order to put the model (1) into perspective let us for a moment focus on a simplified version of (1) where (i) convective terms are disregarded; (ii) the second equation is simplified by neglecting the adsorption isotherm  $a(c)$  and using the approximation  $sc \approx c$  (assuming that  $s$  does not become too small and that the concentration  $c$  is small). Consequently, the following model is obtained

$$\begin{aligned} s_t &= \varepsilon([-\lambda_o f](s, c)P_c(s, c))_x \\ c_t &= \delta(D(s)c_x) + \varepsilon(c[-\lambda_o f](s, c)P_c(s, c))_x. \end{aligned} \quad (3)$$

A characteristic feature of this model is that the equations are strongly coupled in the sense that the parabolic equation for  $s$  contains second derivatives both of  $s_{xx}$  and  $c_{xx}$ . Similarly, the same is true for the second equation describing the dynamics of  $c$ . In particular, the  $c_{xx}$  term in the first equation and the  $s_{xx}$  term in the second equation is often referred to as *cross-diffusion* terms. It is pointed out in several recent papers that the inclusion of such terms make models more realistic since they can incorporate important new effects however at the cost of making the analysis of such models much more difficult. Interesting examples (among many others) of such models relevant for porous media flow are given in [14, 13, 16, 15]. Another example is the well-known Keller-Segel model used to describe the collective motion of biologic cells, see for example [17, 18] and references therein. Another area which applies models involving strongly coupled diffusion terms as in (3) is modelling of cancer cell dynamics [19]. Finally, various models relevant for mathematical biology which involve both triangular diffusion matrix (only one of the equations involve cross-diffusion) as well as full diffusion matrix (both equations involve cross-diffusion) are investigated in [20, 21].

On this background it seems clear that the model (1) requires careful investigations. Especially, some aspects of the following points will be addressed in this work:

- (i) What is characteristic behavior for the solutions?
- (ii) To what extent can important effects relevant for dynamic wettability alteration be captured by the proposed model, in view of observations from experiments?
- (iii) What is the role played by cross-diffusion terms?

Having derived the model which includes dynamic wettability alteration, a discrete approximation is considered by applying the relaxed scheme [22] for the discretization of the convective terms. A good feature of this scheme is that it gives accurate resolution of sharp fronts. The diffusion terms are treated by standard central discretization. Armed with the numerical scheme an example with a vertical core plug is investigated. The core plug is sealed everywhere except at the top surface leading to countercurrent spontaneous imbibition. Through numerical computations the role of molecular diffusion of the WA agent into the core plug is explored. Similarly, the balance between gravity and capillary forces is illustrated, and comparison

of the performance of the imbibition process with permanent wetting state versus dynamic wettability alteration is studied. In particular, a new and characteristic oil-bank is observed which is due to the incorporation of dynamic wettability alteration. In other words, it cannot be seen for the case with permanent wetting states. This phenomenon is caused by the cross-diffusion term appearing in the capillary diffusion term for the equation for  $s$ .

The paper is organized as follows. In Section 2 the basic mechanism of wettability alteration using interpolation between oil-wet and water-wet relative permeability and capillary pressure curves is introduced. In Section 3 the governing flow equations for mass conservation are presented. Appropriate boundary conditions for counter-current imbibition are stated. In Section 4 discretization of the resulting system of strongly coupled convection-diffusion equations is outlined. In Section 5 various aspects of the model are systematically explored using numerical computations. Both transient and quasi-steady state behavior is studied.

**2. Modelling of wettability alteration.** The aim is to build a mathematical model which can be used to study spontaneous imbibition processes on laboratory scale. More precisely, focus is on a spontaneous imbibition process for a core plug surrounded by seawater as indicated by Fig. 1. It is sealed everywhere except at the top, thus, seawater can only enter from the top. In the following the seawater phase is represented by the saturation variable  $s$ , whereas  $c$  is used to represent the concentration of a wettability alteration (WA) agent. Before developing the model in detail it is useful to summarize by words, based on insight from previous studies [1]–[9], the main mechanisms of spontaneous imbibition owing to dynamic wettability alteration:

*An initial oil-wet core plug is given with an initial constant water distribution  $s_{w,initial}$  such that the corresponding capillary pressure  $P_c(s_{w,initial})$  is negative. Consequently, no spontaneous imbibition of water will take place. The mechanism to initiate the process is molecular diffusion of the wettability alteration (WA) agent into the core from the surrounding seawater phase. As the WA agent is absorbed on the rock, the wetting state is rendered to be locally water-wet. Consequently, the capillary pressure  $P_c(s_{w,initial})$  becomes positive in the corresponding part of the core, thereby creating spontaneous imbibition. The dynamics of the resulting imbibition process is then determined by an internal interplay between capillary forces, gravity, adsorption, and molecular diffusion.*

In order to develop a model that can describe this process, appropriate relative permeability curves and capillary pressure curves must be defined that can represent the wetting state of the core plug. In the following it is assumed that the core plug initially is filled with 25% water, i.e.  $s_{init} = 0.25$ , and that the core initially is oil-wet. Below two sets of curves for relative permeability ( $k_r^{ow}, k_r^{ww}$ ) and capillary pressure ( $P_c^{ow}, P_c^{ww}$ ) are specified, corresponding to oil-wet and water-wet conditions. Idealized and simplistic curves are used since this work is meant to be a first study of basic mechanisms related to dynamic wettability alteration rather than providing direct comparisons with experimental data [23, 24].

**2.1. Relative permeability and capillary pressure functions.** As a basic model the well-known Corey type correlations are used [25]. They are given in

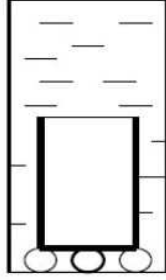


FIGURE 1. Schematic figure for the spontaneous imbibition process on laboratory scale.

the form (dimensionless functions)

$$\begin{aligned} k(s) &= k^* \left( \frac{s - s_{wr}}{1 - s_{or} - s_{wr}} \right)^{Nk}, & s_{wr} \leq s \leq 1 - s_{or}, \\ k_o(s) &= k_o^* \left( \frac{1 - s_{or} - s}{1 - s_{or} - s_{wr}} \right)^{Nk_o}, & s_{wr} \leq s \leq 1 - s_{or}, \end{aligned} \quad (4)$$

where  $s_{wr}$  and  $s_{or}$  represent critical saturation values and  $Nk$  and  $Nk_o$  are the Corey exponents that must be specified. In addition,  $k^*$  and  $k_o^*$  are the end point relative permeability values that also must be given.

As a simple model for capillary pressure a piecewise linear function of the following form is used

$$P_c(s) = C^* \begin{cases} 1 & s < s_{wr}, \\ 1 + \left( \frac{pc_1 - 1}{s_1 - s_{wr}} \right) (s - s_{wr}) & s_{wr} \leq s \leq s_1, \\ pc_1 + \left( \frac{pc_2 - pc_1}{s_2 - s_1} \right) (s - s_1) & s_1 \leq s \leq s_2, \\ pc_2 + \left( \frac{-1 - pc_2}{s_{or} - s_2} \right) (s - s_2) & s_2 \leq s \leq 1 - s_{or}, \\ -1 & s > 1 - s_{or}, \end{cases} \quad (5)$$

where  $C^*$  and the points  $(s_1, pc_1)$  and  $(s_2, pc_2)$  are constants that must be specified. In a more realistic setting these would be based on experimental data and, typically, more than two points would be given. Furthermore,  $C^*$  is a scaling constant (characteristic capillary pressure) that contains information about interfacial tension and contact angle effects. More precisely,  $P_c(s) = C^* J(s)$ , where the dimensionless function  $J(s)$  is called the Leverett function and its multiplier  $C^*$  takes the form [10]

$$C^* = \frac{\sigma \cos(\theta)}{\sqrt{K/\phi}}, \quad (6)$$

where  $\sigma$  is interfacial tension,  $\theta$  is contact angle,  $K$  absolute permeability,  $\phi$  porosity. In the following data required to obtain concrete relative permeability and capillary pressure curves are specified that can represent, respectively, oil-wet and water-wet conditions.

**Oil-wet conditions.** The following set of values for *oil-wet* conditions is used:

$$k^{*,ow} = 0.7, \quad k_o^{*,ow} = 0.75, \quad s_{wr}^{ow} = 0.1, \quad s_{or}^{ow} = 0.15, \quad Nk^{ow} = 2, \quad Nk_o^{ow} = 3. \quad (7)$$

Applying these values in (4) the following two relative permeability curves are obtained

$$k^{ow}(s; s_{wr}^{ow}, s_{or}^{ow}), \quad k_o^{ow}(s; s_{wr}^{ow}, s_{or}^{ow}), \quad \text{for } s_{wr}^{ow} \leq s \leq 1 - s_{or}^{ow}.$$

Similarly, from (5) a corresponding capillary pressure function is obtained

$$P_c^{ow}(s; s_{wr}^{ow}, s_{or}^{ow}), \quad \text{for } s_{wr}^{ow} \leq s \leq 1 - s_{or}^{ow},$$

where the following values are used

$$(s_1^{ow}, pc_1^{ow}) = (0.2, -0.1), \quad (s_2^{ow}, pc_2^{ow}) = (0.8, -0.5). \quad (8)$$

Moreover,  $C^*$  is associated with a reference capillary pressure value which we denote by  $P_{c,r}$

$$C^{*,ow} = P_{c,r}. \quad (9)$$

A specific value for  $P_{c,r}$  is given in Section 5.1. We refer to Fig. 2 for a plot of these curves (red line). In particular, note that  $P_c^{ow}(s_{\text{init}}) < 0$  for  $s_{\text{init}} = 0.25$  which implies that no spontaneous imbibition can take place for this wetting state.

**Water-wet conditions.** The following set of values for *water-wet* conditions is used:

$$k^{*,ww} = 0.4, \quad k_o^{*,ww} = 0.9, \quad s_{wr}^{ww} = 0.15, \quad s_{or}^{ww} = 0.25, \quad Nk^{ww} = 3, \quad Nk_o^{ww} = 2. \quad (10)$$

These choices give corresponding relative permeability curves

$$k^{ww}(s; s_{wr}^{ww}, s_{or}^{ww}), \quad k_o^{ww}(s; s_{wr}^{ww}, s_{or}^{ww}), \quad \text{for } s_{wr}^{ww} \leq s \leq 1 - s_{or}^{ww},$$

and via (5) a corresponding capillary pressure function

$$P_c^{ww}(s; s_{wr}^{ww}, s_{or}^{ww}), \quad \text{for } s_{wr}^{ww} \leq s \leq 1 - s_{or}^{ww},$$

with

$$(s_1^{ww}, pc_1^{ww}) = (0.2, 0.4), \quad (s_2^{ww}, pc_2^{ww}) = (0.7, -0.3). \quad (11)$$

Again

$$C^{*,ww} = P_{c,r}. \quad (12)$$

We refer to Fig. 2 for a plot of these curves (blue line). In particular, note that  $P_c^{ww}(s_{\text{init}}) > 0$  for  $s_{\text{init}} = 0.25$  which implies that spontaneous imbibition will take place for this wetting state.

**2.2. Molecular diffusion and adsorption.** Molecular diffusion of the WA agent is thought to be responsible for the initial wettability alteration. Typical expression for molecular diffusion is of the form

$$D(s) = D_r g(\phi, s), \quad g(\phi, s) = \phi s, \quad (13)$$

where  $D_r$  is a characteristic molecular diffusion coefficient and  $\phi$  is porosity of the porous media. As the the WA agent diffuses into the core it will be absorbed on the rock and this, in turn, brings forth the wettability alteration towards more water-wet conditions. The adsorption effect of the WA agent is taken into account via an adsorption isotherm  $a(c)$  which depends on the concentration  $c$  of the wettability

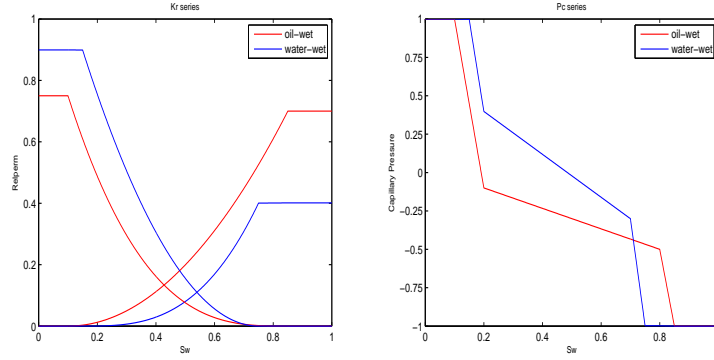


FIGURE 2. **Left:** Example of relative permeability curves corresponding to oil-wet and water-wet conditions. **Right:** Example of capillary pressure curves corresponding to oil-wet and water-wet like conditions.

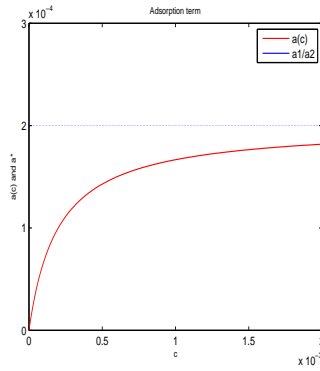


FIGURE 3. The adsorption coefficient  $a(c)$  and its asymptotic limit  $a^*$ .

alteration (WA) agent. More precisely, a Langmuir type adsorption isotherm [10] is used given in the form

$$a(c) = \frac{a_1 c}{1 + a_2 c}, \quad a_1, a_2 > 0, \quad (14)$$

where  $a_1, a_2$  are specified constants. In the remaining part of the paper we use  $a(c)$  given by

$$a(c) = \frac{c}{1 + 5000c}, \quad (15)$$

i.e.,  $a_1 = 1$  and  $a_2 = 5000$ .

**2.3. Modelling of transition from oil-wet to water-wet conditions.** Improved oil recovery by invasion of seawater in an initially oil-wet porous medium is ultimately due to changes in various flow parameters. The flow conditions before and after the wettability alteration can be described by capillary pressure curves, relative permeability curves, and residual saturations. In this work wettability alteration is incorporated in these flow parameters by defining capillary pressure  $P_c(s, c)$

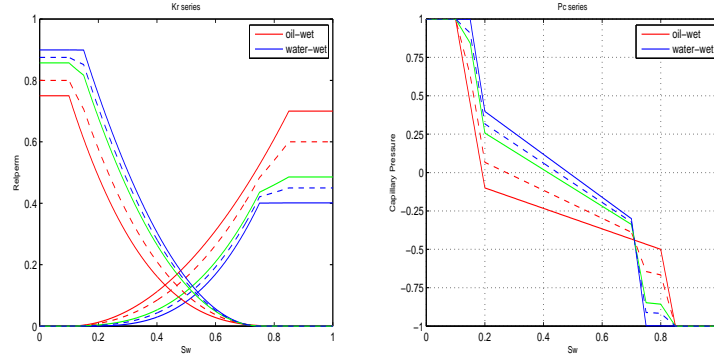


FIGURE 4. Relative permeability curves (left) and capillary curves (right) corresponding to oil-wet ( $c = 0$ ), intermediate wet ( $c = 0.0001, c = 0.0005, c = 0.001$ ), and water-wet like conditions ( $c = 0.05$ ), respectively, by using the interpolation (16)–(18) with  $a(c)$  given by (15).

and relative permeability curves  $k(s, c), k_o(s, c)$  through an interpolation between the oil-wet and water-wet curves given in (4)–(12).

More precisely, motivated by the fact that transition from oil-wet towards water-wet conditions depends on the adsorption of the WA agent on the rock through the adsorption isotherm  $a(c)$ , the following interpolation is proposed:

$$k(s, c) = F(c)k^{ow}(s) + [1 - F(c)]k^{ww}(s), \quad (16)$$

where  $F(c)$  is assumed to depend on  $a(c)$  in the following manner:

$$F(c) = \frac{a^* - a(c)}{a^*}, \quad a^* = \frac{a_1}{a_2}, \quad (17)$$

and  $a^*$  is the asymptotic limit of  $a(c)$ . Clearly,  $0 \leq F(c) \leq 1$ . Furthermore, when no adsorption of the WA agent has taken place it follows that  $a(c) = 0$  and  $F(c) = 1$  implying that  $k(s, c) = k^{ow}(s)$ . This reflects the initial oil-wet wetting state. Then, as the WA agent is absorbed on the rock it follows that  $a(c)$  increases towards its asymptotic limit  $a^*$  as described by the curve shown in Fig. 3. In particular, for high enough concentration  $c$  we see that  $a(c) \approx a^*$ . This implies that  $F(c) \approx 0$ , which means that  $k(s, c) \approx k^{ww}(s)$ , reflecting that a wettability alteration has taken place which results in water-wet wetting states. In particular, different concentration values  $c$  produce relative permeability curves that lie between the two extremes  $k^{ow}$  and  $k^{ww}$ , see Fig. 4 (left figure), which shows intermediate wetting states.

The same interpolation procedure is natural to use for the capillary pressure curves. That is,

$$P_c(s, c) = F(c)P_c^{ow}(s) + [1 - F(c)]P_c^{ww}(s). \quad (18)$$

Thus, different concentration values  $c$  produce capillary pressure curves that lie between the two extremes  $P_c^{ow}$  and  $P_c^{ww}$ , see Fig. 4 (right figure).

**3. Governing equations.** In this section the relevant three-component (oil-water-WA agent) system is stated. Non-dimensional versions are identified as well as appropriate initial and boundary conditions.

**3.1. The dynamic wettability alteration (WA) model.** The basic underlying assumption is that we have two phases, water and oil, where water is immiscible with oil. The oil phase involves only one oil component whereas the water phase involves a water component and a WA agent component. Assuming one-dimensional flow in a homogeneous medium, the mass conservation of the three components oil, water, and WA agent, respectively, is given by the following set of equations [10, 25]:

$$(\phi\rho_o s_o)_t + (\rho_o v_o)_x = \rho_o q_o, \quad (19)$$

$$(\phi\rho s[1 - c])_t + (\rho[1 - c]v)_x = \rho q, \quad (20)$$

$$(\phi\rho s c + (1 - \phi)\rho_r a(c))_t + (\rho c v)_x = (\rho D(s)c_x)_x + \rho c q_c. \quad (21)$$

It is assumed that volumes do not change when the WA agent is dissolved in water. The variables  $\rho_o$ ,  $\rho$ , and  $\rho_r$  represent respectively oil, water, and rock density. The variable  $s$  is the saturation of the water phase (the mixture of water and WA agent) which we may refer to as the aqueous phase. The oil phase is denoted by  $s_o$  and is related to  $s$  by  $s_o = 1 - s$ . The variable  $c$  is the concentration of WA agent in the aqueous phase (volumetric fraction in the water phase). Thus,  $s(1 - c)$  represents the volume fraction of the water component whereas  $sc$  represents the volume fraction of the WA agent component. Moreover,  $\phi$  is the porosity, and  $v$  and  $v_o$  denote the volumetric flow rates of the aqueous phase and oil, respectively, whereas  $q_o$ ,  $q$ , and  $q_c$  represent rates of production/injection (in terms of volume per unit time). As described in Section 2.2 the function  $a(c)$  models adsorption of the WA agent on rock whereas  $D(s)$  represents molecular diffusion of seawater ions into the rock pore space and is responsible for initiating the spontaneous imbibition of seawater into an oil-wet rock.

Making the approximation that the volume fraction of the WA agent is negligible compared with the water (setting  $[1 - c] \approx 1$ , see e.g. [26]), (20) takes the form

$$(\phi\rho s)_t + (\rho v)_x = \rho q. \quad (22)$$

In addition we assume incompressible rock and fluids, i.e.  $\rho_o$ ,  $\rho$ , and  $\rho_r$  are independent of pressure, together with the assumption that the water density  $\rho$  is independent of the composition of the water phase represented by  $c$ . Consequently, all densities become constant and the following simplified model is obtained (with a slight abuse of notation since we absorb the term  $\frac{(1-\phi)\rho_r}{\phi\rho}$  in the function  $a(c)$ )

$$\phi(s_o)_t + (v_o)_x = q_o, \quad (23)$$

$$\phi(s)_t + (v)_x = q, \quad (24)$$

$$\phi(sc + a(c))_t + (cv)_x = (D(s)c_x)_x + cq_c. \quad (25)$$

Including gravity, we get  $v$  and  $v_o$  by Darcy's law as follows:

$$v = -K\lambda[(p)_x - \rho g Z'(x)], \quad \lambda(s, c) = \frac{k(s, c)}{\mu} \quad (26)$$

$$v_o = -K\lambda_o[(p_o)_x - \rho_o g Z'(x)], \quad \lambda_o(s, c) = \frac{k_o(s, c)}{\mu_o}, \quad (27)$$

where  $Z(x) = -x$  and positive direction is upward. In the following  $g$  means  $g = -9.81$ .  $K$  represents absolute permeability and is assumed to be constant,  $p$  represents water pressure,  $p_o$  oil pressure, and  $k, k_o$  are relative permeability functions as described in Section 2. The mobilities  $\lambda$  and  $\lambda_o$  are defined in (26) and (27) where the water and oil viscosities  $\mu$  and  $\mu_o$  are assumed to be constant.

Moreover, capillary pressure  $P_c(s, c)$  is defined as the difference between oil and water pressure

$$P_c(s, c) = p_o(c, s) - p(c, s), \quad (28)$$

where  $P_c$  is a known function. Total velocity  $v_T$  is given by

$$\begin{aligned} v_T = v + v_o &= -K \left( \lambda[p_x - \rho g] + \lambda_o[(p_o)_x - \rho_o g] \right) \\ &= -K \left( \lambda[(p_o)_x - (P_c)_x - \rho g] + \lambda_o[(p_o)_x - \rho_o g] \right) \\ &= -K \left( \lambda_T(p_o)_x - \lambda(P_c)_x - g[\lambda\rho + \lambda_o\rho_o] \right) \\ &= -K\lambda_T(p_o)_x + K\lambda(P_c)_x + Kg[\lambda\rho + \lambda_o\rho_o], \end{aligned} \quad (29)$$

where total mobility  $\lambda_T$

$$\lambda_T = \lambda + \lambda_o, \quad (30)$$

has been introduced. Summing the equations (23) and (24), and using that  $1 = s + s_o$ , implies that

$$(v_T)_x = q + q_o.$$

Assuming that  $q = q_o = 0$  (no mass inflow/outflow associated with the two phases), i.e.,  $v_T = \text{constant}$  and is determined from boundary conditions. From (29) it follows that

$$p_o = \int^x \frac{1}{\lambda_T} \left( \lambda(P_c)_x + g[\lambda\rho + \lambda_o\rho_o] - \frac{v_T}{K} \right) dx, \quad (31)$$

which can be used to obtain  $p_o$  once  $s$  and  $c$  are known. From the continuity equation for  $s$  given by (24) it follows (since  $v = -K\lambda[(p_o)_x - (P_c)_x - \rho g]$ )

$$\phi s_t + \left( -K\lambda(p_o)_x \right)_x + \left( K\lambda(P_c)_x \right)_x + \left( K\lambda\rho g \right)_x = 0, \quad (32)$$

where, in view of (29),

$$-K(p_o)_x = \frac{v_T}{\lambda_T} - K \frac{\lambda}{\lambda_T} (P_c)_x - Kg \left[ \frac{\lambda}{\lambda_T} \rho + \frac{\lambda_o}{\lambda_T} \rho_o \right].$$

Thus,

$$\begin{aligned} \phi s_t + \left( \lambda \left[ \frac{v_T}{\lambda_T} - K \frac{\lambda}{\lambda_T} (P_c)_x - Kg \left[ \frac{\lambda}{\lambda_T} \rho + \frac{\lambda_o}{\lambda_T} \rho_o \right] \right] \right)_x \\ + \left( K\lambda(P_c)_x \right)_x + \left( K\lambda\rho g \right)_x = 0. \end{aligned} \quad (33)$$

The fractional flow function  $f(s, c)$  and  $f_o(s, c)$  are defined as follows

$$f(s, c) \stackrel{\text{def}}{=} \frac{\lambda(s, c)}{\lambda(s, c) + \lambda_o(s, c)}, \quad (34)$$

$$f_o(s, c) \stackrel{\text{def}}{=} \frac{\lambda_o(s, c)}{\lambda(s, c) + \lambda_o(s, c)} = 1 - f(s, c). \quad (35)$$

Using this in (33) implies that

$$\phi s_t + \left( v_T f(s, c) + Kg \Delta\rho [f\lambda_o](s, c) \right)_x - \left( K[\lambda f](s, c)(P_c)_x - K\lambda(s, c)(P_c)_x \right)_x = 0, \quad (36)$$

where  $\Delta\rho = [\rho - \rho_o]$ . Noting from (34) that

$$\lambda f - \lambda = -\lambda_o f,$$

(36) can be written in the form

$$\phi s_t + \left( v_T f(s, c) + \Delta \rho K g [f \lambda_0](s, c) \right)_x = - \left( K [\lambda_o f](s, c) (P_c(s, c))_x \right)_x. \quad (37)$$

The same procedure can be applied for the continuity equation for the WA agent component given by (25) which gives the following equation:

$$\begin{aligned} \phi [sc + a(c)]_t + \left( c \left[ v_T f(s, c) + \Delta \rho K g [f \lambda_0](s, c) \right] \right)_x \\ = (D(s)c_x)_x - \left( K c [\lambda_o f](s, c) (P_c(s, c))_x \right)_x, \end{aligned} \quad (38)$$

where it has been assumed that  $q_c = 0$ . Thus, in view of (37) and (38), a model has been obtained of the form

$$\begin{aligned} \phi s_t + v_T \left( f(s, c) + G [f \lambda_o](s, c) \right)_x \\ = (B_1(s, c)s_x)_x + (B_2(s, c)c_x)_x, \end{aligned} \quad (39)$$

$$\begin{aligned} \phi [sc + a(c)]_t + v_T \left( c \left[ f(s, c) + G [f \lambda_o](s, c) \right] \right)_x \\ = (D(s)c_x)_x + (cB_1(s, c)s_x)_x + (cB_2(s, c)c_x)_x, \end{aligned} \quad (40)$$

where  $G$  is a constant given by  $G = \Delta \rho K (g/v_T)$ ,  $f(s, c)$  is given by (34) whereas the diffusion coefficients  $B_1(s, c)$  and  $B_2(s, c)$ , are given by

$$B_1(s, c) = -K \lambda_o(s, c) f(s, c) (P_c)_s, \quad B_2(s, c) = -K \lambda_o(s, c) f(s, c) (P_c)_c. \quad (41)$$

**Remark 1.** Note that the model (39)–(40) is included as a special case of the general formulation used in [10] (chapter 5) where a 1-D model for displacement of oil by water with chemical components is studied. However, the aim of the current work is to study the effects from capillary diffusion and gravity on laboratory scale, whereas main focus in [10] is on reservoir scale simulations where molecular diffusion, capillary diffusion, and gravity are disregarded.

**Remark 2.** Concerning the impact from the molecular diffusion term  $(D(s)c_x)_x$  in (40) it is expected that for small times this term plays an important role for an initial oil-wet core plug where the concentration  $c$  initially is zero. In fact, the molecular diffusion is responsible for initiating the whole spontaneous imbibition of seawater into the core plug. At later times the performance of the imbibition process is a result of an intricate interplay between various forces; gravity, capillary diffusion, and viscous forces. See Section 5 for more details.

**Remark 3.** Assuming that the total velocity  $v_T = 0$  the model (39) and (40) takes the simpler form

$$\phi s_t + \left( \Delta \rho K g [f \lambda_o](s, c) \right)_x = (B_1(s, c)s_x)_x + (B_2(s, c)c_x)_x, \quad (42)$$

$$\begin{aligned} \phi [sc + a(c)]_t + \left( c \left[ \Delta \rho K g [f \lambda_o](s, c) \right] \right)_x \\ = (D(s)c_x)_x + (cB_1(s, c)s_x)_x + (cB_2(s, c)c_x)_x. \end{aligned} \quad (43)$$

In particular, neglecting gravity a pure nonlinear and coupled diffusion system of the form

$$\phi s_t = (B_1(s, c)s_x)_x + (B_2(s, c)c_x)_x, \quad (44)$$

$$\phi [sc + a(c)]_t = (D(s)c_x)_x + (cB_1(s, c)s_x)_x + (cB_2(s, c)c_x)_x, \quad (45)$$

is obtained.

**Remark 4** (More components). A more general model may be studied where several components have been included

$$(\phi\rho_0s_0)_t + (\rho_0v_0)_x = \rho_0q_0, \quad (46)$$

$$(\phi\rho s[1-c])_t + (\rho[1-c]v)_x = \rho q, \quad (47)$$

$$(\phi\rho sc_i + (1-\phi)\rho_r a_i(c))_t + (\rho c_i v)_x = (\rho D_i(s)c_{i,x})_x + \rho c_i q_{c_i}, \quad i = 1, 2, \dots, m-1, \quad (48)$$

where  $c = \sum_{i=1}^{m-1} c_i$  and  $c_m = 1 - c$  (equivalently  $\sum_{i=1}^m c_i = 1$ ) and  $c_i \geq 0$ . Consequently, (39) is obtained as before (except that it now depends on  $c_1, \dots, c_{m-1}$ ) and a new convection-diffusion equation of the form (40) is added for each component  $c_i$ .

**Remark 5.** Neglecting capillary pressure effects, i.e.  $P_c = 0$ , as well as the molecular diffusion term  $(D(c)c_x)_x$  gives the hyperbolic system of conservation laws

$$\phi s_t + v_T f(s, c)_x = 0, \quad (49)$$

$$\phi[sc + a(c)]_t + v_T[cf(s, c)]_x = 0. \quad (50)$$

Formally, this model is similar to the model used for polymer flooding [26, 11, 12, 10].

**3.2. Non-dimensional form of the model (39)–(40) with  $v_T \neq 0$  (viscous forces included).** In order to solve the system numerically, we first of all non-dimensionalise the equations. The variables and parameters in the model and their associated boundary conditions are transformed into dimensionless quantities using the following reference variables:

- (i) reference length scale,  $L$  (cm);
- (ii) reference time unit,  $\tau = \frac{\phi L}{v_T}$  (sec);
- (iii) reference molecular diffusion coefficient  $D_r$  ( $\text{m}^2/\text{s}$ ), reference capillary pressure  $P_{c,r}$  (Pa), and reference viscosity  $\mu_r$  (Pa s).

We use the coordinate transformation

$$x' = \frac{x}{L}, \quad t' = \frac{t}{\tau}, \quad (51)$$

and new parameters are defined via the following scaling:

$$D' = \frac{D}{D_r}, \quad \mu' = \frac{\mu}{\mu_r}, \quad P'_c = \frac{P_c}{P_{c,r}} \quad (52)$$

Then the model (39)–(40) takes the form (omitting the prime notation)

$$s_t + f_T(s, c)_x = \varepsilon [B_1(s, c)s_x + B_2(s, c)c_x]_x, \quad \varepsilon = \frac{KP_{c,r}}{Lv_T\mu_r}, \quad \delta = \frac{D_r}{Lv_T} \quad (53)$$

$$[sc + a(c)]_t + [cf_T(s, c)]_x = \delta(D(s)c_x)_x + \varepsilon [cB_1(s, c)s_x + cB_2(s, c)c_x]_x, \quad (54)$$

with

$$f_T(s, c) = f(s, c) + \gamma[f\lambda_o](s, c), \quad \gamma = \frac{\Delta\rho Kg}{v_T\mu_r}, \quad (55)$$

and

$$D(s) = \phi s, \quad B_1(s, c) = -[\lambda_o f](s, c)(P_c)_s, \quad B_2(s, c) = -[\lambda_o f](s, c)(P_c)_c. \quad (56)$$

The dimensionless, characteristic numbers  $\varepsilon$  and  $\gamma$  are sometimes referred to as, respectively, the *capillary number* and *gravity number*. Note also that  $\lambda_o$  and  $P_c$  now refer to dimensionless functions.

For construction of numerical solutions we consider the model in the form

$$s_t + f_T(s, c)_x = \varepsilon \left[ (B_1(s, c)s_x)_x + (B_2(s, c)c_x)_x \right], \quad (57)$$

$$m_t + [cf_T(s, c)]_x = \delta(D(s)c_x)_x + \varepsilon \left[ (cB_1(s, c)s_x)_x + (cB_2(s, c)c_x)_x \right],$$

where  $c$  solves the equation  $m = sc + a(c)$ . Typically this amounts to finding roots of a second order polynomial. In particular, by using the expression (14) for the adsorption, we see that finding  $c$  from  $m = sc + a(c)$  and  $s$  results in the second order polynomial

$$Ac^2 + Bc + C = 0, \quad A(s) = a_2s, \quad B(s, m) = s + a_1 - a_2m, \quad C(m) = -m.$$

Then

$$c = \psi(s, m) = \frac{-B(s, m) + \sqrt{B(s, m)^2 - 4A(s)C(m)}}{2A(s)}. \quad (58)$$

In other words, we can express the  $c$  variable by  $c = \psi(s, m)$ .

**3.3. Non-dimensional form of the model (39)–(40) with  $v_T = 0$  (counter-current flow).** The starting point is the model (42)–(43). Again we use the scaling (51) and (52), the only difference is that a modified characteristic time is used

- (ii) reference time unit,  $\tau = \frac{\phi L^2}{D_r}$  sec where  $D_r$  is the reference chemical (molecular) diffusion coefficient.

Using this scaling the model now takes the form

$$s_t + \gamma f_T(s, c)_x = \varepsilon \left[ (B_1(s, c)s_x)_x + (B_2(s, c)c_x)_x \right], \quad (59)$$

$$[sc + a(c)]_t + \gamma [cf_T(s, c)]_x = \delta(D(s)c_x)_x + \varepsilon \left[ (cB_1(s, c)s_x)_x + (cB_2(s, c)c_x)_x \right], \quad (60)$$

with

$$\gamma = \frac{L\Delta\rho Kg}{\mu_r D_r}, \quad \varepsilon = \frac{KP_{c,r}}{\mu_r D_r}, \quad \delta = 1, \quad (61)$$

where  $f_T(s, c) = [f\lambda_o](s, c)$ . Neglecting gravity gives the pure diffusion model

$$s_t = \varepsilon \left[ (B_1(s, c)s_x)_x + (B_2(s, c)c_x)_x \right], \quad (62)$$

$$[sc + a(c)]_t = \delta(D(s)c_x)_x + \varepsilon \left[ (cB_1(s, c)s_x)_x + (cB_2(s, c)c_x)_x \right], \quad (63)$$

with

$$D(s) = \phi s, \quad B_1(s, c) = -[\lambda_o f](s, c)(P_c)_s, \quad B_2(s, c) = -[\lambda_o f](s, c)(P_c)_c. \quad (64)$$

**Remark 6.** Note that the capillary diffusion coefficients  $B_1$  and  $B_2$  involve  $(P_c)_s$  and  $(P_c)_c$ , respectively. These are given by

$$\frac{\partial P_c}{\partial s}(s, c) = F(c) \frac{d}{ds} P_c^{ow}(s) + [1 - F(c)] \frac{d}{ds} P_c^{ww}(s) \quad (65)$$

and

$$\frac{\partial P_c}{\partial c}(s, c) = F'(c) \left[ P_c^{ow}(s) - P_c^{ww}(s) \right], \quad F'(c) = -\frac{a_2}{a_1} a'(c). \quad (66)$$

The capillary diffusion term associated with  $B_1$  in (53) (and (59)) is similar to the one appearing in a standard Buckley-Leverett two-phase type model (but now with an additional dependence on  $c$ ). However, the diffusion like term associated with  $B_2$  is a consequence of the dynamic wettability alteration and add new effects

to a standard two-phase model with permanent wetting states. In particular, it represents what is sometimes referred to as cross-diffusion [14, 16, 15, 20, 21]. The role of this term is explored in Section 5. The strength of the term  $B_2$  depends on  $(P_c)_c$ . From (66) it is clear that this in turn depends on  $a'(c)$  and  $\Delta P_c = P_c^{ow} - P_c^{ww}$ . Note that  $a'(c)$  contains information about how fast the salt is adsorbed on the rock. In particular,  $a'(0) = \max(a'(c))$  where  $a'(c)$  tends to zero as  $c$  increases. This follows from

$$h(c) = a'(c) = \frac{a_1}{1 + a_2c} - \frac{a_1 a_2 c}{(1 + a_2c)^2}. \quad (67)$$

Clearly, the  $B_2$ -term impacts in an interval starting at the front of the WA agent where  $a'(c)$  takes its largest value and where, at the same time, there is a gradient in the concentration of the WA agent,  $c_x \neq 0$ . As  $c$  becomes larger,  $a'(c)$  goes to zero, and the effect from the  $B_2$ -related capillary diffusion term vanishes. For further discussion, see Section 5.6.

**3.4. Boundary and initial conditions.** In the remaining part of this work we shall restrict ourselves to the case with spontaneous counter-current imbibition. Consequently, the bottom of the core is sealed, only the top is open. When the plug is closed at the bottom the total velocity  $v_T$  at the bottom vanishes, i.e.  $v_T = 0$ , which means that we consider the model (59)–(60).

**Bottom.** It is clear that there is no mass flux at the bottom. That is, the total flux (convective and diffusive) is zero at the bottom which corresponds to the following boundary condition, see e.g. [28] for a similar situation,

$$\begin{aligned} \gamma f_T(c, s) - \varepsilon [B_1(s, c)s_x + B_2(s, c)c_x] &= 0, & \text{for } x = 0 \\ \gamma [cf_T(c, s)] - \varepsilon [D(s)c_x + cB_1(s, c)s_x + cB_2(s, c)c_x] &= 0, & \text{for } x = 0. \end{aligned} \quad (68)$$

**Top.** The top is open, and an appropriate boundary condition must be specified. Since the top surface is exposed to seawater with a specified concentration of the WA agent, it is natural to use the Dirichlet condition

$$s(1^+, t) = 1.0, \quad c(1^+, t) = c^*, \quad (69)$$

where  $c^*$  is the specified concentration of the WA agent in the seawater. In addition we also have the boundary condition

$$P_c(t)|_{x=1^+} = 0, \quad (70)$$

which implies that the capillary diffusion term causes flow of seawater into the core plug only if  $P_c(s, c)|_{x=1^-} > 0$ .

Using (69) and (70) we can specify the total flux at the top surface for the water phase equation (59). On the other hand if  $P_c(s, c)|_{x=1^-} \leq 0$  the model, through its capillary term, tries to move water out of the plug through the top end. However, there is no oil available outside the plug that can replace this water. Consequently, the total flux at the top must be set to zero. The only thing that can happen then is a redistribution of the water phase  $s$  within the core due to gravity.

Concerning the equation (60) for the WA concentration  $c$  it is assumed that molecular diffusion is the only force that makes the WA agent enter at the top surface. In other words, we use the condition that

$$\gamma [cf_T(c, s)] - \varepsilon [cB_1(s, c)s_x + cB_2(s, c)c_x] = 0, \quad \text{for } x = 1. \quad (71)$$

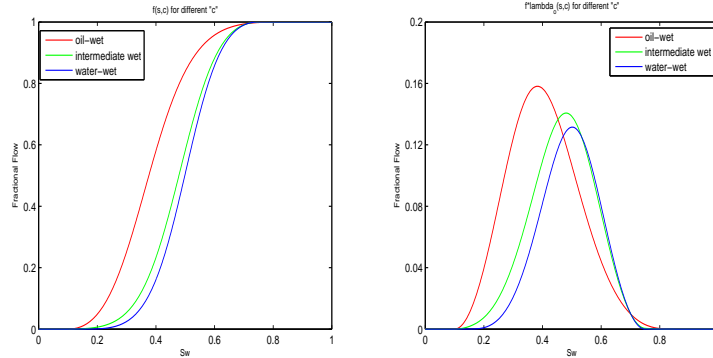


FIGURE 5. The fractional flow function  $f_T(s, c)$  in (55) is composed of  $f(s, c)$  (left) associated with viscous forces and  $[f\lambda_o](s, c)$  (right) associated with gravitation. Different curves are shown corresponding to oil-wet ( $c = 0$ ), intermediate wet ( $c = 0.001$ ), and water-wet like conditions ( $c = 0.05$ ), respectively, by using the interpolation (16) and (17) with  $a(c)$  given by (15).

**Initial data.** Initially, the plug is filled with oil and 25% formation water and it is surrounded by seawater. Thus, initial data are given by

$$s(x, 0) = 0.25, \quad c(x, 0) = 0, \quad x \in [0, 1].$$

**4. Discrete approximation.** Since pressure is decoupled from the calculation of  $s$  and  $c$  through (31), the main purpose is to solve a 2x2 system of equations of the general form

$$u_t + f(u)_x = (a(u)u_x)_x, \quad u(x, 0) = u_0(x). \quad (72)$$

In order to study solutions of this simplified model the relaxed scheme proposed by Jin and Xin [22] is employed for the numerical discretization of the *convective fluxes*. This scheme, which has been tested for many different hyperbolic conservation laws, see for instance [27] and references therein, is known to be robust and accurate for many cases without using any information about the eigenstructure associated with  $f(u)$ .

For the discretization of the *diffusive fluxes* of the convection-diffusion system a straightforward “central in space-explicit in time” type of discretization is employed. It is well known that this imposes a somewhat strict CFL condition on the time step. However, since efficiency of the numerical calculations is not the main aim of the present investigations but seeking insight into fundamental mechanisms relevant for wettability alteration processes, a simple explicit in time discretization is preferred for both the convective and diffusive fluxes. In this respect we also follow along the line of, for instance [28] (which apply a discretization similar to the one proposed in [29]) where the Kurganov-Tadmor central-upwind scheme has been used for the convective part together with a central type discretization of the diffusive part.

First, for the domain  $Q_T = [0, 1] \times [0, T]$  a uniform grid in space and time is assumed. That is, for  $K$  spatial cells of length  $\Delta x = 1/K$  we associate  $x_{j+1/2}$  with cell interface for  $j = 0, \dots, K$  and  $x_j$  with cell center for  $j = 1, \dots, K$ . Similarly,

for  $N$  temporal time steps of length  $\Delta t = 1/N$  we have  $t^n = n\Delta t$  for  $n = 1, \dots, N$ . A discrete version (finite volume type) of (72) is then given by

$$\frac{U_j^{n+1} - U_j^n}{\Delta t} + \frac{1}{\Delta x} \left( F_{j+1/2}^n - F_{j-1/2}^n \right) = \frac{1}{\Delta x} \left( a_{j+1/2}^n D_+ U_j^n - a_{j-1/2}^n D_- U_j^n \right), \quad (73)$$

where  $F_{j+1/2}^n = F(U_j^n, U_{j+1}^n)$  is a numerical flux to be specified whereas the diffusion coefficient  $a_{j+1/2}^n = a(U_j^n, U_{j+1}^n)$  represents an appropriate average at the interface  $j + 1/2$ . We shall apply an arithmetic average. Here the notation  $D_+ U_j = (U_{j+1} - U_j)/\Delta x$  and  $D_- U_j = (U_j - U_{j-1})/\Delta x$  is used. We note that there is a CFL stability condition associated with the explicit time discretization used in (73) of the form [28]

$$\frac{\Delta t}{\Delta x} \max_u \rho[Df(u)] + \frac{\Delta t}{2\Delta x^2} \max_u \rho[a(u)] \leq \frac{1}{4}, \quad (74)$$

where  $Df(u)$  denotes the Jacobian matrix associated with the flux  $f(u)$  and  $\rho$  represents the spectral radius.

**4.1. Discretization in the interior domain.** The model we focus on takes a form slightly different from (72). More precisely, in view of (57) the model can be written in the form

$$\begin{aligned} s_t + f_T(c, s)_x &= \varepsilon \left[ -(\lambda_o f)(s, c) P_c(s, c)_x \right]_x, & f_T &= f + \lambda_o f, \\ m_t + [cf_T(c, s)]_x &= \delta (D(s)c_x)_x + \varepsilon \left[ -c(\lambda_o f)(s, c) P_c(s, c)_x \right]_x, \end{aligned} \quad (75)$$

where  $c = \psi(s, m)$  as described in (58). Thus, a discretization of the following form is employed for  $j = 2, \dots, K - 1$ :

$$\begin{aligned} & \frac{S_j^{n+1} - S_j^n}{\Delta t} + \frac{1}{\Delta x} \left( [F_T]_{j+1/2}^n - [F_T]_{j-1/2}^n \right) \\ &= \frac{\varepsilon}{\Delta x} \left( [-\lambda_o f]_{j+1/2}^n D_+ [P_c]_j^n - [-\lambda_o f]_{j-1/2}^n D_- [P_c]_j^n \right), \\ & \frac{M_j^{n+1} - M_j^n}{\Delta t} + \frac{1}{\Delta x} \left( [cF_T]_{j+1/2}^n - [cF_T]_{j-1/2}^n \right) \\ &= \frac{\delta}{\Delta x} \left( [D]_{j+1/2}^n D_+ c_j^n - [D]_{j-1/2}^n D_- c_j^n \right) \\ & \quad + \frac{\varepsilon}{\Delta x} \left( [-c\lambda_o f]_{j+1/2}^n D_+ [P_c]_j^n - [-c\lambda_o f]_{j-1/2}^n D_- [P_c]_j^n \right). \end{aligned} \quad (76)$$

We refer to Appendix A for details concerning the discrete convective fluxes  $[F_T]_{j+1/2}^n$  and  $[cF_T]_{j+1/2}^n$  appearing in (76). This approach gives a second-order, conservative central type finite volume scheme for the convective transport associated with (75) similar to the approach used, for instance, in [28, 30]. Higher order accuracy could also be implemented along the line of [31, 32] (see also references therein).

The relaxed scheme requires only information about the maximal eigenvalue associated with the flux vector  $(f(c, s), cf(s, c))$ . For that purpose we note that the left-hand side of (75) can be written as

$$u_t + A(u)u_x = 0, \quad A(u) = \begin{pmatrix} f_s(s, c) & f_c(s, c) \\ 0 & \frac{f(s, c)}{s+h(c)} \end{pmatrix},$$

where  $u = (s, c)$  [11]. This follows by first observing that the model can be written as

$$B(u)u_t + C(u)u_x = 0, \quad B(u) = \begin{pmatrix} 1 & 0 \\ c & [s + a'(c)] \end{pmatrix}, \quad C(u) = \begin{pmatrix} f_s & f_c \\ cf_s & [f + cf_c] \end{pmatrix},$$

and

$$B^{-1}(u) = \begin{pmatrix} 1 & 0 \\ -\frac{c}{s+h} & \frac{1}{s+h} \end{pmatrix}.$$

Eigenvalues are then given by

$$\lambda^s = f_s, \quad \lambda^c = \frac{f}{s + h(c)}, \quad \text{where } h(c) = a'(c). \quad (77)$$

**Remark 7.** In the work [28] no special conditions are enforced when discretizing the diffusion term of (73) whereas the authors of [30] enforce certain continuity conditions as a part of their mixed-finite element discretization approach. In order to make calculations more efficient one could also use an operator splitting (fractional-step) approach where the convection-diffusion system is split into a separate convection and diffusion step.

**4.2. Discretization at the boundary.** The discretization (76) is used in the interior of the core plug domain, i.e., for cell  $j = 2, \dots, K - 1$ . Below we describe the discretization at cell  $j = 1$  and  $j = K$  corresponding to the bottom cell and top cell.

**Bottom: Cell  $j = 1$ .** In view of the boundary conditions (68) and the discrete scheme (76) we consider the following scheme for cell  $j = 1$ .

$$\begin{aligned} & \frac{S_1^{n+1} - S_1^n}{\Delta t} + \frac{1}{\Delta x} \left( [F_T]_{1+1/2}^n - 0 \right) \\ & \quad = \frac{\varepsilon}{\Delta x} \left( [-\lambda_o f]_{1+1/2}^n D_+ [P_c]_1^n - 0 \right), \\ & \frac{M_1^{n+1} - M_1^n}{\Delta t} + \frac{1}{\Delta x} \left( [cF_T]_{1+1/2}^n - 0 \right) \\ & \quad = \frac{\delta}{\Delta x} \left( [D]_{1+1/2}^n D_+ c_1^n - 0 \right) + \frac{\varepsilon}{\Delta x} \left( [-c\lambda_o f]_{1+1/2}^n D_+ [P_c]_1^n - 0 \right). \end{aligned} \quad (78)$$

**Top: Cell  $j = K$ .** An additional cell (ghost cell)  $j = K + 1$  is introduced at the top. In view of the boundary conditions (69) and (70), we set

$$S_{K+1}^n = 1.0, \quad C_{K+1}^n = c^*, \quad [P_c]_{K+1}^n = 0,$$

for all  $n$ , which allows to calculate the flux  $[F_T]_{K+1/2}^n$ , coefficient  $[-\lambda_o f]_{K+1/2}^n$  and discrete derivative  $D_+ [P_c]_K^n$ . Together with (71), which is applied for the second equation of (76), the scheme takes the following form for cell  $j = K$ :

$$\begin{aligned} & \frac{S_K^{n+1} - S_K^n}{\Delta t} + \frac{1}{\Delta x} \left( [F_T]_{K+1/2}^n - [F_T]_{K-1/2}^n \right) \\ & \quad = \frac{\varepsilon}{\Delta x} \left( [-\lambda_o f]_{K+1/2}^n D_+ [P_c]_K^n - [-\lambda_o f]_{K-1/2}^n D_- [P_c]_K^n \right), \\ & \frac{M_K^{n+1} - M_K^n}{\Delta t} + \frac{1}{\Delta x} \left( 0 - [cF_T]_{K-1/2}^n \right) \\ & \quad = \frac{\delta}{\Delta x} \left( [D]_{K+1/2}^n D_+ c_K^n - [D]_{K-1/2}^n D_- c_K^n \right) + \frac{\varepsilon}{\Delta x} \left( 0 - [-c\lambda_o f]_{K-1/2}^n D_- [P_c]_K^n \right). \end{aligned} \quad (79)$$

**5. Simulation cases.** Through various numerical computations we will explore the role of molecular diffusion of the WA agent into the core plug, the balance between gravity and capillary forces, and dynamic wettability alteration versus permanent wetting state for a case with spontaneous counter-current imbibition. First we specify some data needed for the simulations. These are used throughout all simulations if nothing else is said.

5.1. **Various data.** Data we use are as follows:

**Core plug properties.**

- Length of core plug:  $L = 4.0$  cm.
- Permeability:  $K = 5$  mD  $= 5 \cdot 0.987 \cdot 10^{-15}$  m<sup>2</sup>.
- Porosity:  $\phi = 0.4$ .

**Oil properties.**

- Oil viscosity:  $\mu_o = 0.6$  cp (1 cp =  $10^{-3}$  Pa s)
- Oil density :  $\rho_o = 0.73$  g/cm<sup>3</sup>

**Brine properties.**

- Water viscosity:  $\mu = 0.3$  cp
- Water density:  $\rho = 0.92$  g/cm<sup>3</sup>
- Concentration of WA agent:  $c^* = 0.001$ .

Salt concentration  $c_s$  in sea water is taken to be:  $c_s = 0.024$  mol/l = 2.3 g/l. Assuming that the density of salt is  $\rho_s = 2.68$  g/cm<sup>3</sup>, it follows that the corresponding volumetric fraction of salt in seawater is  $c = \frac{2.30}{2.68} 10^{-3} = 0.8582 \cdot 10^{-3} \approx 10^{-3}$ .

**Other quantities.**

- Reference molecular diffusion:  $D_r = 5 \cdot 10^{-10}$  m<sup>2</sup>/s.
- Reference capillary pressure:  $P_{c,r} = 3 \cdot 10^2$  Pa.
- Reference viscosity:  $\mu_r = 10^{-3}$  Pa s.

Oil recovery is defined as

$$\text{Oil Recovery} := \frac{\int_0^1 [s(x,t) - s_{\text{init}}(x)] dx}{\int_0^1 [1 - s_{\text{init}}(x)] dx},$$

where  $s_{\text{init}}(x)$  is initial water saturation in the core. All simulations are run on a grid with 80 cells. Grid refinement shows that this is sufficient to give an accurate approximation. Note that since we apply an explicit time discretization of the diffusion terms, in view of (74), we have to deal with a rather strict CFL condition. Therefore, we seek to avoid using too many grid cells. For all simulations we have used a time step determined by the rough estimate

$$\Delta t = 0.95 \frac{\Delta x^2}{\varepsilon},$$

which has been sufficient to ensure that (74) is satisfied.

**5.2. Example 1: Characteristics of seawater imbibition with dynamic wettability alteration.** Figs. 6 and 7 show the distribution of the WA agent concentration  $c$ , capillary pressure  $P_c$  and water saturation  $s$  plotted along  $x$ -axis for different times. Note that the right-hand side of the figures corresponds to the top of the core plug. Fig. 6 focus on small times and reflects that molecular diffusion initiates the transport of the WA agent into the initially oil-wet core from the top (left figure). The WA agent is absorbed onto the rock surface rendering the surface to be more water-wet. This is reflected by the middle plot showing that capillary pressure becomes positive at the top of the core. In turn, this leads to imbibition of seawater (right figure), and a corresponding production of oil.

Fig. 7 shows the distribution of  $c$ ,  $P_c$ , and  $s$  in the core after  $T = 3$  days. Most notably, we observe from the right figure (water phase  $s$ ) that an oil-bank has formed which is surrounded by a left and right-hand water front. This can be explained as follows: The left figure shows that the WA agent has reached approximately the center of the core. A corresponding wettability alteration has taken place in the upper part of the core leading to positive capillary pressure (middle figure). As a consequence, capillary diffusion becomes the driving force in this part of the core and is responsible for the right-hand water front. The bottom part of the core is still oil-wet and capillary pressure is negative. Hence, capillary forces do not contribute here, however, due to gravity another water front is formed. This indicates that there is an interaction between gravity and capillarity which is characteristic for the performance of the imbibition process.

Next, we see from Fig. 8 that after 80 days, the imbibition process has arrived quasi steady state. The WA agent is almost uniformly distributed inside the core (left figure) which means that the core now is completely water-wet. The negative capillary pressure (middle figure) tells us that capillary diffusion does not contribute any longer, gravity is the dominating force in the final stage of the imbibition process. This is also clearly reflected by the distribution of  $s$  (right figure) whose negative slope is due to gravity alone. Finally, Fig. 9 shows the oil recovery through a period of 80 days and reflects that most of the oil has been produced after 30-40 days.

**5.3. Example 2: The role of molecular diffusion of the WA-agent.** Capillary forces cannot drive seawater into the core since it initially is oil-wet (which implies that capillary pressure is negative). At this stage molecular diffusion plays a crucial role as it initiates the diffusion of the WA agent into the core, independent of capillary forces. In the current example the role of molecular diffusion for the imbibition process is explored by considering different values for the coefficient  $D_r$ .

Results for three different values of  $D_r$  are shown in Fig. 10 after  $T = 3$  days. The left plot illustrates that enhancing molecular diffusion by increasing  $D_r$  will lead to a stronger transport effect of the WA agent into the core. This in turn speeds up the wettability alteration caused by the WA agent and the corresponding imbibition of seawater into the core, see right figure for the water distribution  $s$ .

Fig. 11, showing oil recovery curves for the different choices of  $D_r$ , also reflects that the effect of increasing  $D_r$  is a higher oil recovery in the initial period. However, after long enough time when the WA agent concentration has arrived at the same value throughout the core and the degree of wettability alteration is largely the same, oil recovery tends to the same highest value independent of the different molecular diffusion coefficients. In particular, different choices of  $D_r$  do not

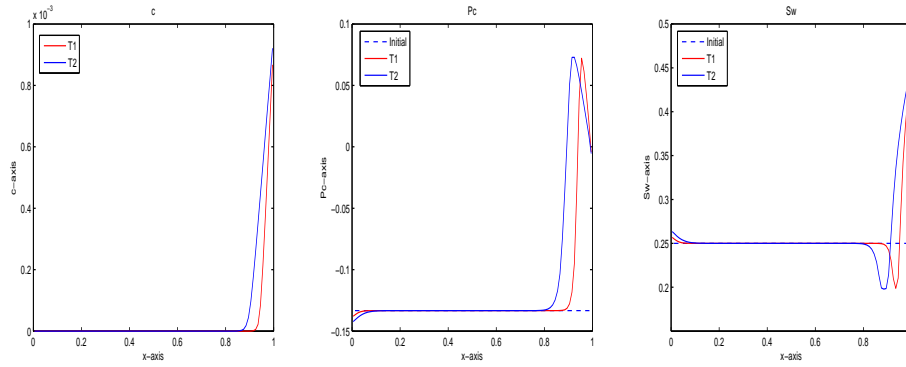


FIGURE 6. **Left:** WA agent concentration  $c$  inside the core after  $T_1 = 1$  hour and  $T_2 = 3$  hours. **Middle:** Corresponding capillary pressure  $P_c$  distribution. **Right:** Corresponding water phase  $s$  distribution.

The plots show how the imbibition process is initiated by the diffusion of the WA agent into the core from top, and the corresponding adsorption onto the rock, which brings forth a wettability alteration towards more water-wet conditions. Consequently, capillary pressure  $P_c$  becomes positive at the top, and the imbibition of seawater starts.

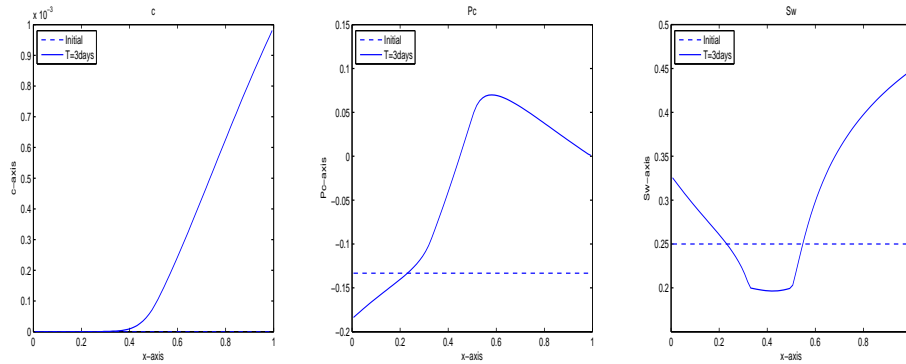


FIGURE 7. The plots show the imbibition process after  $T = 3$  days. **Left:** WA agent concentration  $c$ . **Middle:** Capillary pressure  $P_c$  distribution. **Right:** Water phase  $s$  distribution.

directly affect the balance between gravity and capillarity which can be seen from the expression for  $\gamma$  and  $\varepsilon$  given by (61).

**5.4. Example 3: The balance between gravity and capillarity.** Figs. 12–13 show solutions after time  $T = 3$ , and  $T = 80$  days where we compare results, respectively, with and without gravity influence. That is, we compare results produced respectively by the model (59)–(60) and (62)–(63). First, it is observed from left-hand figure of Fig. 12 that the transport of the WA agent to a large extent is

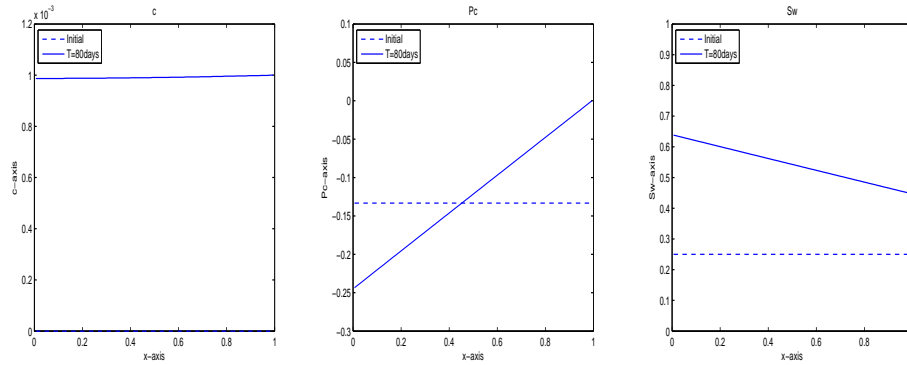


FIGURE 8. The plots show the imbibition process after  $T = 80$  days when a steady state like situation has been reached. **Left:** WA agent concentration  $c$ . **Middle:** Capillary pressure  $P_c$  distribution. **Right:** Water phase  $s$  distribution.

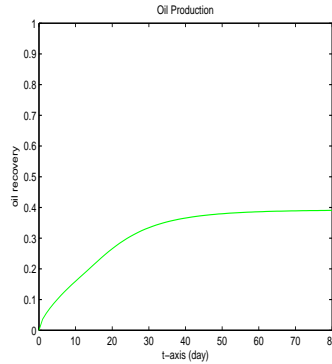


FIGURE 9. Oil recovery through a period of 80 days.

the same for both cases after  $T = 3$  days. Consequently, the wettability alteration is largely the same. From the right figure for the water phase we see that the right-hand water front due to capillary forces is then very similar for both cases. The main difference lies in the treatment of the oil-bank. When gravity is neglected, the negative capillary pressure in the lower part of the core implies that the oil-bank is trapped. However, when gravity is included accumulation of water at the bottom leads to another water front on the left side of the oil-bank. The interaction between the left and right water wave then leads to a much more efficient release of the oil bank, as can be seen from the oil recovery plots in Fig. 14.

The steady state type of solutions shown in Fig. 13 reflect that the water-wet state is the same for both cases after  $T = 80$  days (left figure showing the concentration  $c$ ), however gravity works independent of capillary diffusion and imbibes water despite the fact that capillary pressure is negative throughout the core (see middle figure of Fig. 13). Thus, the final water distribution is given by a straight line whose slope depends on the strength of gravity versus capillary forces, see right figure of Fig. 13.

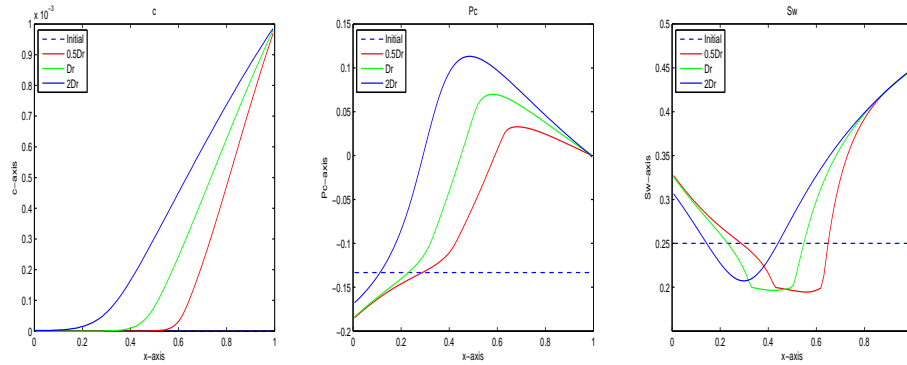


FIGURE 10. We consider the situation after 3 days of imbibition with different molecular diffusion coefficients corresponding to  $D_r = 5 \cdot 10^{-10} \text{ m}^2/\text{s}$  (green),  $0.5D_r$  (red), and  $2D_r$  (blue). **Left:** WA agent concentration  $c$ . **Middle:** Capillary pressure  $P_c$  distribution. **Right:** Water phase  $s$  distribution.

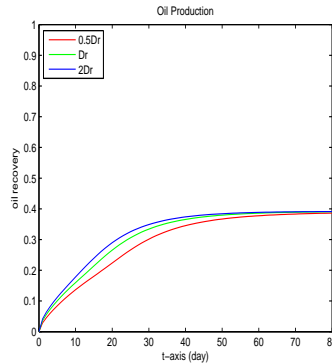


FIGURE 11. Oil recovery after 80 days imbibition with different molecular diffusion coefficients  $D_r = 5 \cdot 10^{-10} \text{ m}^2/\text{s}$  (green),  $0.5D_r$  (red), and  $2D_r$  (blue).

In Figs. 15–17 the balance between gravity and capillary diffusion is altered, represented by  $\gamma$  and  $\varepsilon$  in (61), by changing the reference capillary pressure value  $P_{c,r}$ . Hence, in addition to standard  $P_{c,r}$  value, two other cases are considered corresponding to  $0.5P_{c,r}$  and  $2P_{c,r}$ . Left figure of Fig. 15 reflects that the degree of wettability alteration is the same, practically speaking. The right figure of Fig. 15 clearly indicates that the interplay between the left and right water front (which is crucial for the release of the oil-bank) is clearly affected by considering different  $P_{c,r}$  values, i.e., by changing the balance between gravity and capillarity. In particular, by increasing  $P_{c,r}$ , the right water front (due to capillary forces) becomes larger whereas the left (due to gravity) becomes smaller.

Fig. 17 reflects that the balance between gravity and capillarity becomes important for the oil recovery at later times, e.g. after 25 days. Clearly, gravity is crucial for the later stage of the imbibition process and oil recovery increases with a more

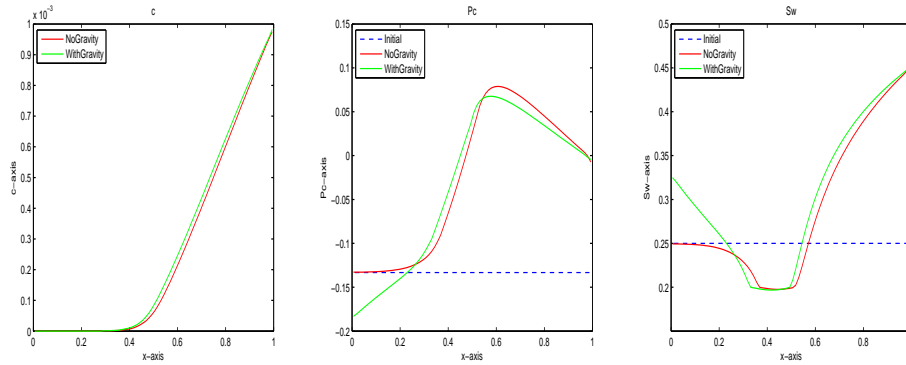


FIGURE 12. The plots show the imbibition process after  $T = 3$  days. **Left:** WA agent concentration  $c$ . **Middle:** Capillary pressure  $P_c$  distribution. **Right:** Water phase  $s$  distribution.

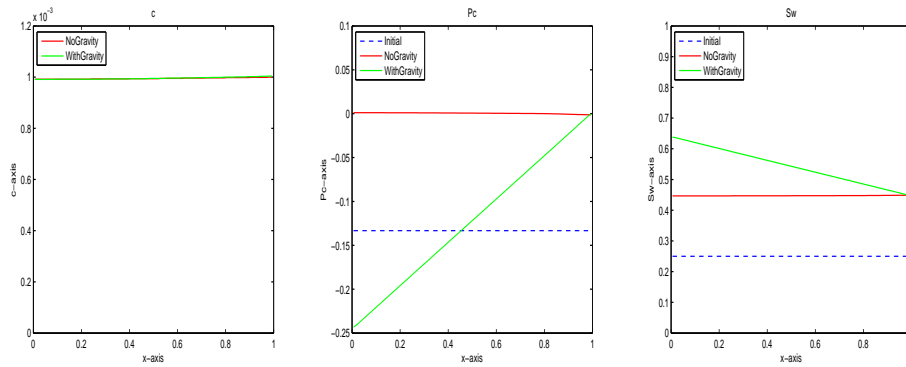


FIGURE 13. The plots show the imbibition process after  $T = 80$  day when a steady state like situation has been reached. **Left:** WA agent concentration  $c$ . **Middle:** Capillary pressure  $P_c$  distribution. **Right:** Water phase  $s$  distribution.

dominating gravity force. This is also reflected by Fig. 16 showing steady state solutions after  $T = 80$  days.

**5.5. Example 4: Dynamic wettability alteration versus permanent wetting states.** The purpose of this example is to compare solutions obtained by the model (59)–(60) and a standard Buckley-Leverett two-phase model with permanent wetting characteristics. More precisely, we compare the model (59)–(60) with the simplified model

$$s_t + \gamma f_T(c, s)_x = \varepsilon \left[ (B_1(s, c)s_x)_x + (B_2(s, c)c_x)_x \right],$$

$$c = c^*,$$

where  $c^*$  is a fixed value. In other words, we consider the two-phase Buckley-Leverett model

$$s_t + \gamma f_T(c^*, s)_x = \varepsilon (B_1(s, c^*)s_x)_x. \quad (80)$$

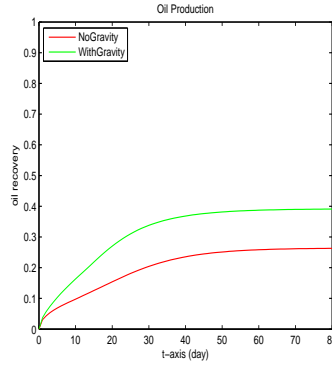


FIGURE 14. Oil recovery after 80 days imbibition with gravity and without gravity influence.

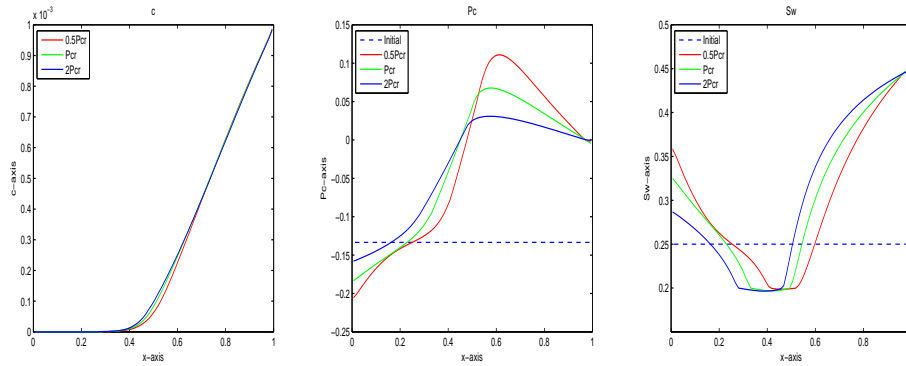


FIGURE 15. The plots show the imbibition process after  $T = 3$  days with different  $P_{c,r}$  values corresponding to  $P_{c,r} = 3 \cdot 10^2$  Pa (green),  $0.5P_{c,r}$  (red), and  $2P_{c,r}$  (blue). **Left:** WA agent concentration  $c$ . **Middle:** Capillary pressure  $P_c$  distribution. **Right:** Water phase  $s$  distribution.

The choice of  $c^*$  will then determine the wetting state of the core, i.e., which relative permeability curve and capillary pressure curve that are used. First, we run simulations where the model (80) with three different  $c^*$  values is considered,  $c_1^* = 0.0001$ ,  $c_2^* = 0.001$ , and  $c_3^* = 0.01$ . See Fig. 18 for the corresponding relative permeability and capillary pressure curves. Results for three different times  $T_1 = 1$  day,  $T_2 = 3$  days, and  $T_3 = 80$  days are shown in Fig. 19 (water distribution  $s$ ) and 20 (capillary pressure distribution  $P_c$ ). Clearly, more water-wet conditions leads to more imbibition of water (thus, a higher oil recovery).

Next, results produced by the model (59)–(60) with dynamic WA together with standard data (those used in Example 1) are compared with results produced by the model (80) with permanent water-wet conditions corresponding to  $c^* = 0.001$ . See Fig. 21 for the curves that are used. Results are shown in Figs. 22–25 for times  $T = 1$  hour,  $T = 1$  day,  $T = 3$  days, and  $T = 80$  days, respectively. Oil recovery is shown in Fig. 26. Figs. 22–25 show that dynamic wettability alteration from oil-wet

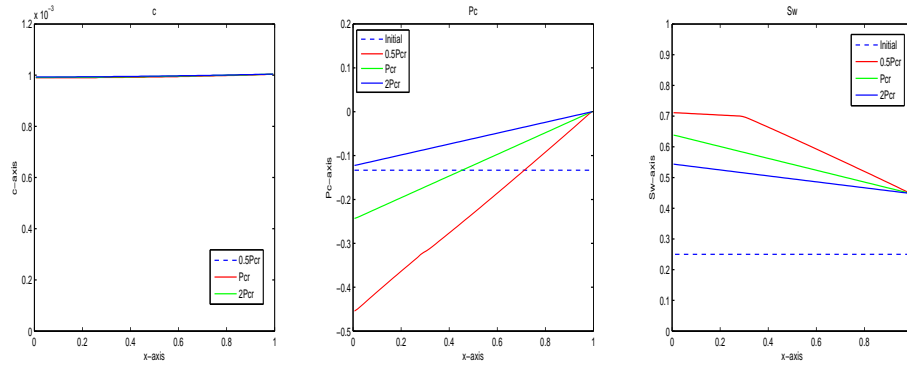


FIGURE 16. The plots show the imbibition process after  $T = 80$  days with different  $P_{c,r}$  values corresponding to  $P_{c,r} = 3 \cdot 10^2$  Pa (green),  $0.5P_{c,r}$  (red), and  $2P_{c,r}$  (blue). **Left:** WA agent concentration  $c$ . **Middle:** Capillary pressure  $P_c$  distribution. **Right:** Water phase  $s$  distribution.

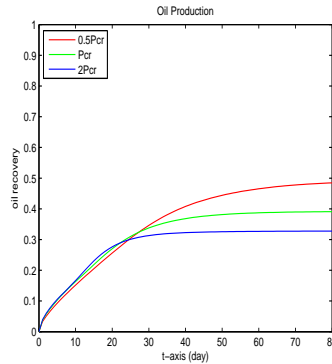


FIGURE 17. Oil recovery after 80 days with different  $P_{c,r}$  values.

towards water-wet conditions produces a behavior that is fundamentally different from the case with permanent wettability conditions. This is clearly seen from the right figure of Figs. 22, 23 and 24. Most notably, a new “dip” in the water distribution  $s$  behind the front of the WA agent appears. This oil-bank is formed owing to the inclusion of dynamic wettability alteration. There is also a difference at the bottom region of the core. The  $P_c$  curves show that capillary forces have an impact throughout the whole core ( $P_c$  is positive) for the case with permanent water-wet conditions. In particular, gravity is balanced against capillary diffusion and the water accumulation at the bottom of the core is much weaker than for the case with dynamic WA. For that case capillary forces are absent (since  $P_c$  is negative here) and gravity is the only force at work. Finally, Fig. 25 and 26 reflect that steady-state solutions become very similar for both cases.

**5.6. Example 5: The role of the difference  $\Delta P_c = P_c^{ow} - P_c^{ww}$ .** In the final example we seek insight into the mechanism that produces the new oil-bank. For

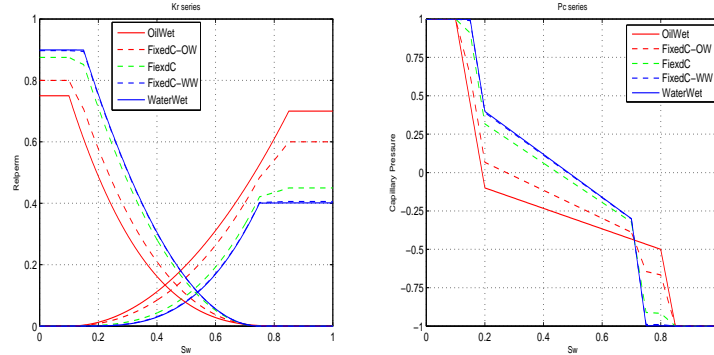


FIGURE 18. Three different relative permeability and capillary pressure curves corresponding to oil-wet conditions  $c_1^* = 0.0001$  (dashed red), intermediate wet conditions  $c_2^* = 0.001$  (dashed green), and water-wet conditions  $c_3^* = 0.01$  (dashed blue). The curves are used for simulations with the model (80) corresponding to permanent wetting states.

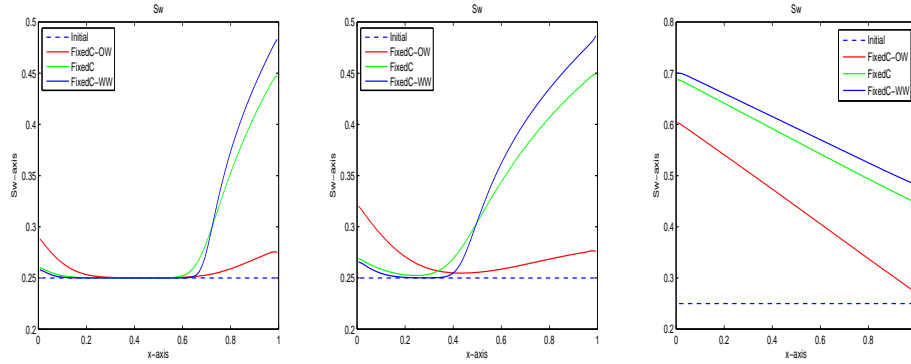


FIGURE 19. Solutions produced by (80) with  $c_1^* = 0.0001$  (solid red),  $c_2^* = 0.001$  (solid green), and  $c_3^* = 0.01$  (solid blue). Water phase  $s$  for different times  $T_1 = 1$  (left),  $T_2 = 3$  (middle), and  $T_3 = 80$  days (right).

that purpose the model (62)–(63) is considered where gravity has been neglected. It is suspected that the oil-bank depends on the quantity  $P_c = P_c^{ow} - P_c^{ww}$ , more precisely, that it is related to the second term on the right-hand side of (62). This term, often referred to as a *cross-diffusion* term (see Remark 6), takes the form

$$(B_2(s, c)c_x)_x, \quad B_2(s, c) = -[\lambda_o f](s, c)F'(c)\Delta P_c(s), \quad F'(c) = -\frac{1}{a^*}a'(c). \quad (81)$$

Recalling that the first term on the right-hand side of (62) corresponds to

$$(B_1(s, c)s_x)_x, \quad \text{where } B_1(s, c) = -[\lambda_o f](s, c)(P_c)_s, \quad (82)$$

we want to change the oil-wet  $P_c$  curve such that the difference  $\Delta P_c(s)$  becomes smaller. More precisely, we consider the couple of capillary pressure curves shown

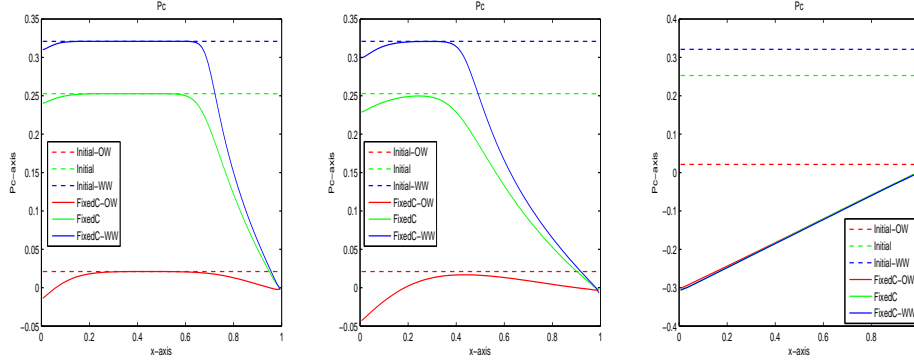


FIGURE 20. Solutions produced by (80) with  $c_1^* = 0.0001$  (solid red),  $c_2^* = 0.001$  (solid green), and  $c_3^* = 0.01$  (solid blue). Capillary pressure  $P_c$  for different times  $T_1 = 1$  (left),  $T_2 = 3$  (middle), and  $T_3 = 80$  days (right).

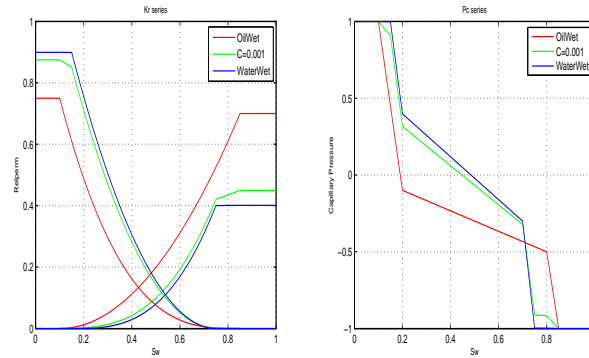


FIGURE 21. Relative permeability curves and capillary pressure curves relevant for the comparison of dynamic wettability alteration versus permanent wettability conditions.

in Fig 27 (referred to as weak cross-diffusion) instead of the previously used couple shown in Fig. 2 (referred to as strong cross-diffusion). From the solutions shown in Fig. 28 it is observed:

- The spreading of the WA agent is very similar independent of the difference in  $\Delta P_c$ .
- The shape of the upper part of the right-hand water wave is very similar for both cases. This must be understood in view of the light that this part of the solution is largely determined by the capillary diffusion term (82). Since the slope of  $P_c(c, s)$  as a function of  $s$ , i.e.  $\partial_s P_c$ , has not been changed (see Fig. 27), we should expect an impact from this term which is similar for both the case with weak and strong cross-diffusion.
- The new dip, which can be seen at the foot of the right water front, clearly seems to be a result of the cross-diffusion term (81). The particular form of

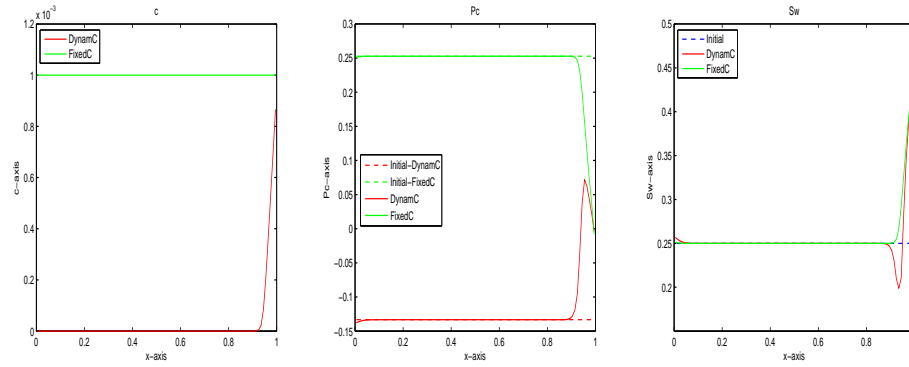


FIGURE 22. Dynamic WA versus permanent wettability conditions,  $T = 1$  hour. **Left:** WA agent concentration  $c$ . **Middle:** Capillary pressure  $P_c$ . **Right:** Water phase  $s$ .

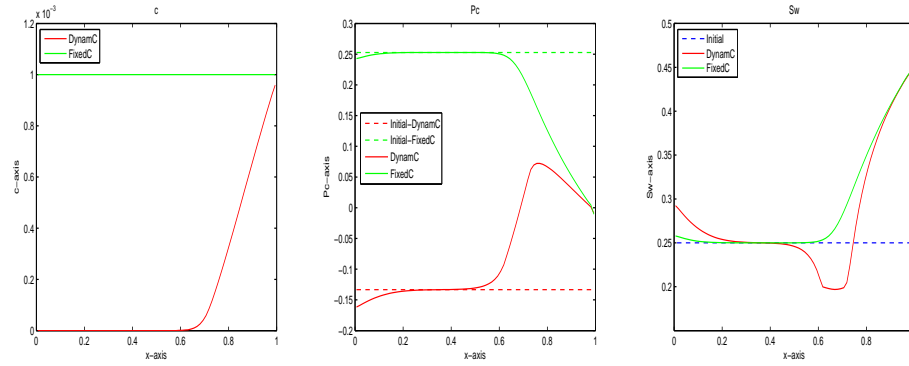


FIGURE 23. Dynamic WA versus permanent wettability conditions,  $T = 1$  day.

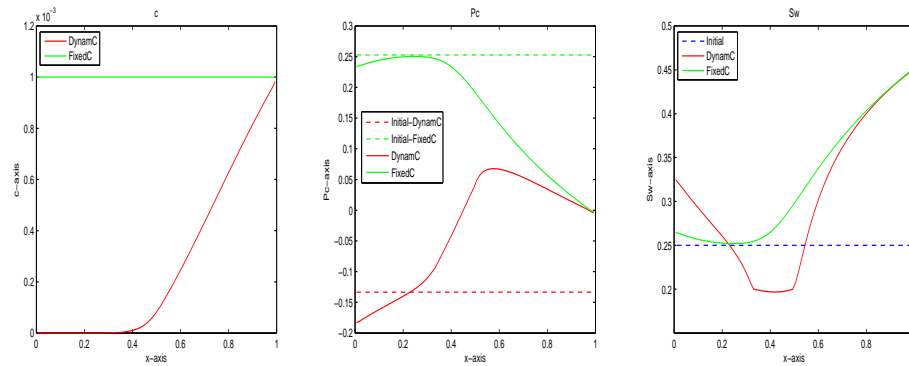


FIGURE 24. Dynamic WA versus permanent wettability conditions,  $T = 3$  day.

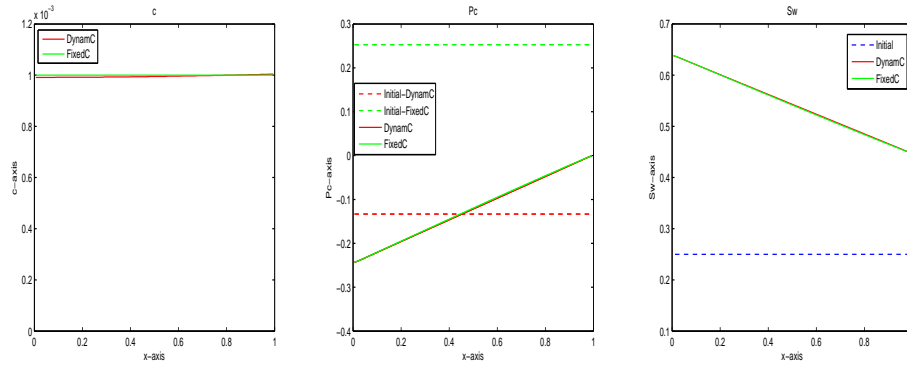


FIGURE 25. Dynamic WA versus permanent wettability conditions,  $T = 80$  days. **Left:** WA agent concentration  $c$ . **Right:** Capillary pressure  $P_c$ . **Bottom:** Water phase  $s_w$ .

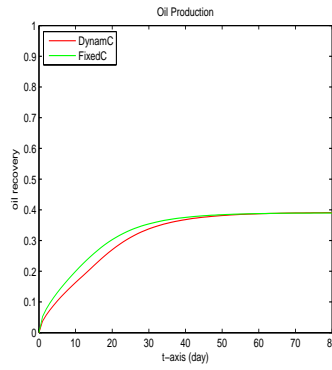


FIGURE 26. Oil recovery during 80 days, respectively, for case with dynamic wettability alteration and permanent wettability conditions.

the coefficient  $B_2(s, c)$  indicates that this term has an impact in an interval that starts at the front of the WA agent concentration (where both  $a'(c) > 0$  and  $c_x \neq 0$  simultaneously) and ends where  $a'(c)$  becomes small (see Fig. 3). See also Remark 6. It seems clear that the size of  $\Delta P_c$  determines how large the dip is.

**6. Concluding remarks.** In this work a 1-D model has been proposed that can describe dynamic wettability alteration. The model is based on fundamental principles (mass conservation and Darcy's law) together with a direct and natural modelling of wettability alteration by interpolating between two sets of relative permeability curves and capillary pressure curves, corresponding to oil-wet and water-wet conditions. The interpolation depends on the adsorption isotherm. More precisely, as the adsorption of the WA agent takes place there is a corresponding alteration toward water-wet conditions (in terms of relative permeability and capillary pressure curves).

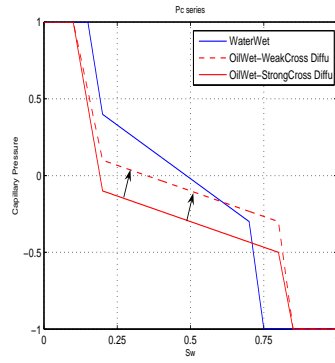


FIGURE 27. Changing the  $P_w^{ow}$  curve towards more water-wet conditions.

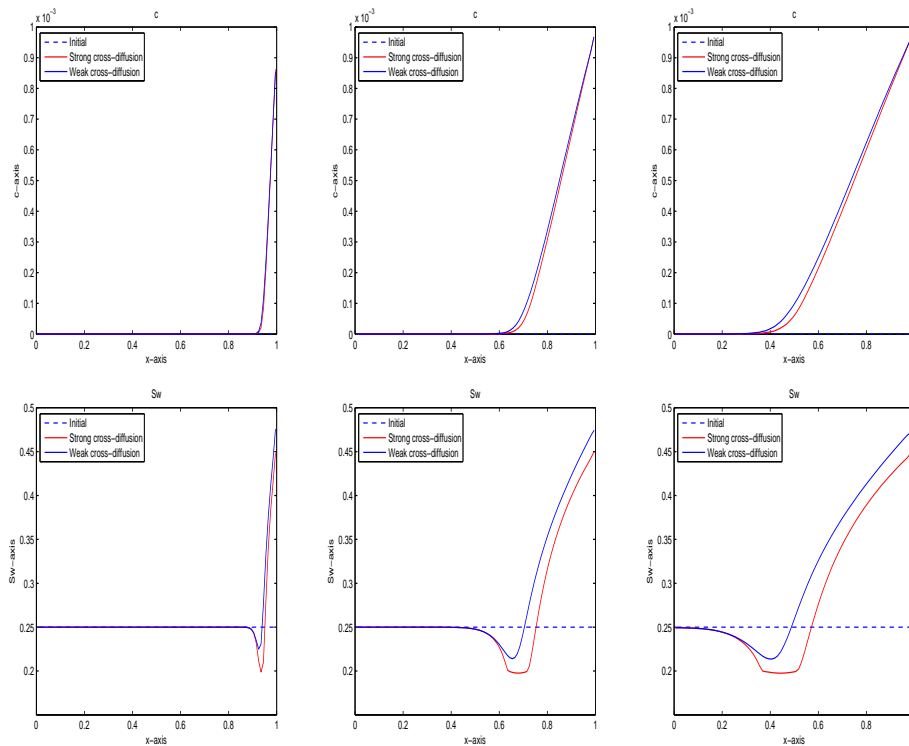


FIGURE 28. Solutions demonstrating how the oil-bank depends on the quantity  $\Delta P_c = P_c^{ow} - P_c^{ww}$ . **Top:** Concentration  $c$  after  $T = 1$  hour (left),  $T = 1$  day (middle), and  $T = 3$  days (right). **Bottom:** Water saturation  $s$  after  $T = 1$  hour,  $T = 1$  day, and  $T = 3$  days.

Characteristic behavior of this model has been investigated by using a numerical discretization procedure. An advantage of the proposed model is that it is not overly complicated, and still it reveals characteristic features due to the inclusion

of dynamic wettability alteration. In particular, (i) the importance of the balance between gravity and capillary forces is clearly demonstrated; (ii) the wave propagation associated with the imbibition process is different compared to simulations with permanent wetting characteristics. A cross-diffusion term, which is related to the difference between oil-wet and water-wet capillary curves, appears in the water phase equation and produces a characteristic effect.

To conclude, there is an essential difference between imbibition with permanent wetting states and dynamic wettability alteration. These results motivate for further work in two directions. Firstly, more experimental work should be done in order to assess the proposed model. Secondly, simplified versions of the model which are more amenable to mathematical analysis and understanding of qualitative properties should also be considered.

### Appendix A: The relaxed scheme.

**The relaxation model for 1-D systems of conservation laws.** Consider now a system of conservation laws in one space variable

$$\partial_t \mathbf{w} + \partial_x F(\mathbf{w}) = Q(\mathbf{w}), \quad (83)$$

where  $F(\mathbf{w}) \in \mathbb{R}^n$  is a smooth vector-valued function. The corresponding relaxation system is then given by

$$\begin{cases} \partial_t \mathbf{w} + \partial_x \mathbf{v} = Q(\mathbf{w}), \\ \partial_t \mathbf{v} + A \partial_x \mathbf{w} = -\frac{1}{\varepsilon}[\mathbf{v} - F(\mathbf{w})], \quad \varepsilon > 0, \end{cases} \quad (84)$$

where

$$A = \text{diag}\{a_1, a_2, \dots, a_n\} \quad (85)$$

is a positive diagonal matrix to be chosen. For small  $\varepsilon$ , applying Chapman-Enskog expansion in the relaxation system (84), one can derive the following approximation for  $\mathbf{w}$  as

$$\partial_t \mathbf{w} + \partial_x F(\mathbf{w}) = Q(\mathbf{w}) + \varepsilon \partial_x (F'(\mathbf{w})Q(\mathbf{w})) + \varepsilon \partial_x ([A - F'(\mathbf{w})^2] \partial_x \mathbf{w}), \quad (86)$$

where  $F'(\mathbf{w})$  is the Jacobian matrix of the flux  $F$ . Equation (86) governs the first-order behavior of the relaxation system (84). Here we must require that the well known subcharacteristic condition holds given by

$$A - F'(\mathbf{w})^2 \geq 0, \quad \text{for all } \mathbf{w}. \quad (87)$$

This condition ensures the dissipative nature of (86). It is clear that for  $\mathbf{w}$  varying in a bounded domain, equation (87) can always be satisfied by choosing sufficiently large  $A$ . However, because of the CFL constraints on numerical stability, it is desirable to obtain the smallest  $A$  meeting the criterion (87). As will be observed in the next section, the size of  $A$  also has a decisive influence regarding the numerical dissipation associated with the numerical schemes derived from (84).

For both theoretical and computational purposes it is sometimes necessary to choose  $A$  to have distinct diagonal elements so as to avoid any degeneracy in the relaxation system. However, for many cases it is sufficient to choose that  $A$  has the special form

$$A = aI, \quad a > 0 \quad (88)$$

where  $I$  is the identity matrix. In the case of one space variable (as we consider) and where we assume (88) the dissipative condition (87) is satisfied if

$$\lambda^2 < a, \quad (89)$$

where  $\lambda = \max_{1 \leq i \leq n} |\lambda_i(\mathbf{w})|$  where  $\lambda_i$  are the genuine eigenvalues of  $F'(\mathbf{w})$ .

**The relaxation schemes.** We will follow the notation of Jin and Xin [22] and use relaxation schemes to denote both the relaxing and relaxed scheme. We recall that the relaxing schemes depend on the relaxation parameter  $\varepsilon$  and the artificial variable  $\mathbf{v}$ , while the zero relaxation limit of these relaxing schemes are the relaxed schemes, independent of both  $\varepsilon$  and  $\mathbf{v}$ .

*The relaxing scheme.* The relaxing scheme associated with the relaxation model (84) is given by

$$\begin{cases} \mathbf{w}_j^{n+1} - \mathbf{w}_j^n + \frac{\lambda}{2}(\mathbf{v}_{j+1}^n - \mathbf{v}_{j-1}^n) - \frac{\lambda}{2}A^{1/2}(\mathbf{w}_{j+1}^n - 2\mathbf{w}_j^n + \mathbf{w}_{j-1}^n) \\ = \Delta t Q(\mathbf{w}_j^n), \\ \mathbf{v}_j^{n+1} - \mathbf{v}_j^n + \frac{\lambda}{2}A(\mathbf{w}_{j+1}^n - \mathbf{w}_{j-1}^n) - \frac{\lambda}{2}A^{1/2}(\mathbf{v}_{j+1}^n - 2\mathbf{v}_j^n + \mathbf{v}_{j-1}^n) \\ = -k(\mathbf{v}_j^{n+1} - F(\mathbf{w}_j^{n+1})), \end{cases} \quad (90)$$

where  $\lambda = \Delta t / \Delta x$  is the mesh ratio, and  $k = \Delta t / \varepsilon$ . Whenever we apply the relaxing scheme for numerical computations, we will use the Runge-Kutta splitting scheme of Jin and Xin which takes two implicit stiff source steps and two explicit convection steps alternatively. We refer to [22] for details on this as well as the second order variant of this scheme.

*The Relaxed Scheme.* Using a formal Hilbert expansion in (90), we get the following relaxed scheme

$$\begin{cases} \mathbf{v}_j^n = F(\mathbf{w}_j^n), \\ \mathbf{w}_j^{n+1} = \mathbf{w}_j^n \\ - \frac{\lambda}{2}(F(\mathbf{w}_{j+1}^n) - F(\mathbf{w}_{j-1}^n)) + \frac{\lambda}{2}A^{1/2}(\mathbf{w}_{j+1}^n - 2\mathbf{w}_j^n + \mathbf{w}_{j-1}^n) + \Delta t Q(\mathbf{w}_j^n). \end{cases} \quad (91)$$

The relaxed scheme can be written on the following ‘‘viscous’’ form

$$\begin{cases} \mathbf{w}_j^{n+1} = \mathbf{w}_j^n - \lambda(\hat{F}_{j+1/2}^n - \hat{F}_{j-1/2}^n) + \Delta t Q(\mathbf{w}_j^n) \\ \text{where} \\ \hat{F}_{j+1/2}^n = \frac{1}{2}(F(\mathbf{w}_j) + F(\mathbf{w}_{j+1})) - \frac{1}{2}A^{1/2}(\mathbf{w}_{j+1} - \mathbf{w}_j), \end{cases} \quad (92)$$

where  $A^{1/2}$  plays the role as the ‘‘viscosity matrix’’ which determines the numerical dissipation of the scheme. The relaxed scheme (91) can also be viewed as a flux splitting scheme. To see this we write the system as

$$\begin{cases} \mathbf{w}_j^{n+1} = \mathbf{w}_j^n - \lambda(\hat{F}_{j+1/2}^n - \hat{F}_{j-1/2}^n) + \Delta t Q(\mathbf{w}_j^n) \\ \text{where} \\ \hat{F}_{j+1/2}^n = F_{j+1/2,-}^+ + F_{j+1/2,+}^-, \end{cases} \quad (93)$$

where we have (for the first order scheme) that

$$F_{j+1/2,-}^+ = F^+(\mathbf{w}_j), \quad F_{j+1/2,+}^- = F^-(\mathbf{w}_{j+1}),$$

and where we have used the Lax-Friedrichs flux splitting

$$F^\pm(\mathbf{w}) = \frac{1}{2}(F(\mathbf{w}) \pm A^{1/2}\mathbf{w}). \quad (94)$$

Note that the condition (87) ensures that the Jacobian of  $F^\pm(\mathbf{w})$  has nonnegative eigenvalues only or nonpositive eigenvalues only.

*Second Order Relaxed Scheme.* The second order relaxed scheme can be obtained by using van Leer's MUSCL scheme. Instead of using the piecewise constant interpolation, the MUSCL uses the piecewise linear interpolation which, applied to the  $p$ -th components of  $F^+(\mathbf{w}_j)$  approximated at  $x_j$  yields:

$$(F^+)_j^{(p)}(x) = (F^+)^{(p)}(\mathbf{w}_j) + (S^+)_j^{(p)}(x - x_j), \quad x \in (x_{j-1/2}, x_{j+1/2})$$

where

$$(S^+)_j^{(p)} = S((s_l^+)^{(p)}, (s_r^+)^{(p)}) \quad (95)$$

and

$$(s_l^+)^p = \frac{(F^+)^{(p)}(\mathbf{w}_j) - (F^+)^{(p)}(\mathbf{w}_{j-1})}{\Delta x}, \quad (s_r^+)^p = \frac{(F^+)^{(p)}(\mathbf{w}_{j+1}) - (F^+)^{(p)}(\mathbf{w}_j)}{\Delta x}.$$

Here  $S(u, v)$  represents the slope limiter function. Similarly, the piecewise linear interpolation applied to the  $p$ -th components of the negative flux part  $F^-(\mathbf{w}_{j+1})$  approximated at  $x_{j+1}$  yields:

$$(F^-)_{j+1}^{(p)}(x) = (F^-)^{(p)}(\mathbf{w}_{j+1}) + (S^-)_{j+1}^{(p)}(x - x_{j+1}), \quad x \in (x_{j+1/2}, x_{j+3/2})$$

where

$$(S^-)_{j+1}^{(p)} = S((s_l^-)^{(p)}, (s_r^-)^{(p)}) \quad (96)$$

and

$$(s_l^-)^p = \frac{(F^-)^{(p)}(\mathbf{w}_{j+1}) - (F^-)^{(p)}(\mathbf{w}_j)}{\Delta x},$$

$$(s_r^-)^p = \frac{(F^-)^{(p)}(\mathbf{w}_{j+2}) - (F^-)^{(p)}(\mathbf{w}_{j+1})}{\Delta x}.$$

The van Leer limiter corresponds to the choice

$$S(u, v) = s(u, v) \frac{2|u||v|}{|u| + |v|}, \quad (97)$$

where  $s(u, v) = 1/2(\text{sgn}(u) + \text{sgn}(v))$ . The numerical flux  $F_{j+1/2}^{(p)}$  is then computed in a split form,

$$\hat{F}_{j+1/2}^{(p)} = (F^+)_j^{(p)}(x)|_{x_{j+1/2}} + (F^-)_{j+1}^{(p)}(x)|_{x_{j+1/2}}. \quad (98)$$

Second order accuracy in time is obtained by using a two-stage Runge-Kutta discretization.

## REFERENCES

- [1] J. E. Sylte, L. D. Hallenbeck and L. K. Thomas, *Ekofisk Formation pilot waterflood*, Paper SPE 18276, presented at the 63th Annual Technical Conference and Exhibition held in Houston, TX, U. S. A., 1988.
- [2] D. C. Standnes and T. Austad, *Wettability alteration in chalk 2. Mechanism for wettability alteration from oil-wet to water-wet using surfactants*, Journal of Petroleum Science and Engineering, **28** (2000), 123–143.
- [3] Strand. Skule, D. C. Standnes and T. Austad, *Spontaneous imbibition of aqueous surfactant solutions into neutral to oil-wet carbonate cores: Effects of brine salinity and composition*, Energy and Fuels, **17** (2000), 1133–1144.
- [4] D. C. Standnes and T. Austad, *Wettability alteration in carbonate interaction between cationic surfactant and carboxylates as a key factor in wettability alteration from oil-wet to water-wet conditions*, Colloids and Surfaces A: Physicochem. Eng. Aspects, **216** (2003), 243–259.
- [5] T. Austad and D. C. Standnes, *Wettability and Oil recovery from Carbonates: Effects of Temperature and Potential Determining Ions*, Journal of Petroleum Science and Engineering, **39** (2003), 363–376.
- [6] T. Austad, S. Strand, E. J. Høegnesen and P. Zhang, *Seawater as IOR fluid in fractured chalk*, Paper SPE 93000, presented at the 2005 SPE International Symposium on Oilfield Chemistry held in Houston, Texas, USA, 2-4 February.
- [7] P. Zhang and T. Austad, *Wettability and oil recovery from carbonates: effects of temperature and potential determining ions*, Colloids and Surfaces A: Physicochem. Eng. Aspects, **279** (2006), 179–187.
- [8] S. Strand, E. J. Høegnesen and T. Austad *Wettability alteration of carbonates effects of potential determining ions ( $Ca^{2+}$  and  $SO_4^{2-}$ ) and temperature*, Colloids and Surfaces A: Physicochem. Eng. Aspects, **275** (2006), 1–10.
- [9] P. Zhang, M. T. Tweheyo and T. Austad, *Wettability alteration and improved oil recovery by spontaneous imbibition of seawater into chalk: Impact of the potential determining ions  $Ca^{2+}$ ,  $Mg^{2+}$ , and  $SO_4^{2-}$* , Colloids and Surfaces A: Physicochem. Eng. Aspects, **301** (2007), 199–208.
- [10] P. Bedrikovetsky, “Mathematical Theory of Oil and Gas Recovery with Applications to ex-USSR Oil and Gas Fields,” Petroleum Engineering & Development Studies, Vol **4**, Kluwer Academic Publishers, 1993.
- [11] T. Johansen and R. Winther, *The solution of the Riemann problem for a hyperbolic system of conservation laws modeling polymer flooding*, SIAM J. Math. Anal., **19** (1988), 541–566.
- [12] T. Johansen and R. Winther, *The Riemann problem for multicomponent polymer flooding*, SIAM J. Math. Anal., **20** (1989), 908–929.
- [13] Y. Amirat and A. Ziani, *Global weak solutions for a parabolic system modeling a one-dimensional miscible flow in porous media*, J. Math. Anal. Appl., **220** (1998), 697–718.
- [14] Y. Amirat and A. Ziani, *Global weak solutions to equations of compressible miscible flows in porous media*, SIAM J. Math. Anal., **38** (2007), 1825–1846.
- [15] H. Frid and V. Shelukhin, *Initial boundary value problems for a quasi-linear parabolic system in three-phase capillary flow in porous media*, SIAM J. Math. Anal., **36** (2005), 1407–1425 (electronic).
- [16] H. Frid and V. Shelukhin, *A quasilinear parabolic system for three-phase capillary flow in porous media*, SIAM J. Math. Anal., **35** (2003), 1029–1041 (electronic).
- [17] B. Perthame, “Transport Equations in Biology,” Frontiers in Mathematics, Birkhauser Verlag, 2007.
- [18] M. Bendahmane, K. H. Karlsen and J. M. Urbano, *On a two-sidedly degenerate chemotaxis model with volume-filling effects*, Math. Models Methods Appl. Sci., **17** (2007), 783–804.
- [19] M. A. J. Chaplain and G. Lolas, *Mathematical modelling of cancer invasion of tissue: Dynamic heterogeneity*, Networks and Heterogeneous Media, **1** (2006), 399–439.
- [20] D. Le and T. T. Nguyen *Persistence for a class of triangular cross diffusion parabolic systems*, Adv. Nonlinear Stud., **5** (2005), 493–514.
- [21] D. Le, *Global existence for a class of strongly coupled parabolic systems*, Annali di Matematica, **185** (2006), 133–154.
- [22] S. Jin and Z. Xin *The relaxation schemes for systems of conservation laws in arbitrary space dimensions*, Comm. Pure Appl. Math., **48** (1995), 235–276.

- [23] S. M. Skjaeveland, L. M. Siqveland, A. Kjosavik, W. L. Hammervold and G. A. Virnovsky, *Capillary pressure correlation for mixed-wet reservoirs*, Paper SPE 77328, presented at the 1998 SPE India Oil and Gas Conference and Exhibition held in New Delhi, India.
- [24] A. Kjosavik, J. K. Ringen and S. M. Skjaeveland, *Relative permeability correlation for mixed-wet reservoirs*, Paper SPE 59314, presented at the 2000 SPE/DOE Improved Oil Recovery Symposium held in Tulsa, Oklahoma, 3-5, 2000.
- [25] Z. Chen, G. Huan and Y. Ma, "Computational Methods for Multiphase Flows in Porous Media," Computational Science & Engineering, SIAM, 2006.
- [26] G. A. Pope, *The application of fractional flow theory to enhanced oil recovery*, Soc. Pet. Engrg. J, **20** (1980), 191-205.
- [27] S. Evje and K. F. Fjelde *Relaxation schemes for the calculation of two-phase flow in pipes*, Math. Comput. Modelling, **36** (2002), 535-567.
- [28] S. Berres, R. Bürger, K. H. Karlsen and E. Tory. *Strongly degenerate parabolic-hyperbolic systems modeling polydisperse sedimentation with compression*, SIAM J. Appl. Math., **64** (2003), 41-80 (electronic).
- [29] A. Kurganov and E. Tadmor, *New high-resolution central schemes for nonlinear conservation laws and convection-diffusion equations*, J. Comput. Phys., **160** (2000), 241-282.
- [30] E. Abreu, J. Douglas Jr., F. Furtado, D. Marchesin and F. Pereira. *Three-phase immiscible displacement in heterogeneous petroleum reservoirs*, Math. Comput. Simulation, **73** (2006), 2-20.
- [31] H. J. Schroll, *Relaxed high resolution schemes for hyperbolic conservation laws*, J. Sci. Comput., **21** (2004), 251-279.
- [32] J. Chen and Z. Shi, *Application of a fourth-order relaxation scheme to hyperbolic systems of conservation laws*, Acta Mech Sinica, **22** (2006), 84-92.

Received September 2007; revised November 2007.

*E-mail address:* liping.yu@uis.no

*E-mail address:* hans.kleppe@uis.no

*E-mail address:* terje.karstad@uis.no

*E-mail address:* s-skj@ux.uis.no

*E-mail address:* steinar.evje@iris.no

*E-mail address:* Ingebret.Fjelde@iris.no